THE CENOZOIC GONYAULACACEAN DINOFLAGELLATE GENERA *OPERCULODINIUM* WALL, 1967 AND *PROTOCERATIUM* BERGH, 1881 AND THEIR PHYLOGENETIC RELATIONSHIPS

by

Manuel Paez-Reyes

A thesis submitted to the Department of Earth Sciences

in partial fulfillment of the requirements for the degree of

Master of Science

Faculty of Mathematics and Science, Brock University

St. Catharines, Ontario

ABSTRACT

The palynology of Ocean Drilling Program Site 1007, leeward of the present Bahamas Bank, provides insights into upper Oligocene–lower Pleistocene dinoflagellate cyst associations in the tropical Americas. These associations are reviewed along with the sedimentary paleoenvironment to provide context for a morphological study of the cyst-defined dinoflagellate *Operculodinium bahamense* and its comparison with the theca-defined dinoflagellate *Protoceratium reticulatum* which produces a cyst assignable to the cyst-defined genus *Operculodinium*. Detailed reconstructions of the tabulation in both species reveal strong similarities, having a sexiform hyposomal tabulation and L-type or modified L-type ventral organization. *Protoceratium reticulatum* has dextral torsion of the hypotheca, requiring assignation of the genus to the subfamily Cribroperidinioideae, whereas *Operculodinium bahamense* has neutral torsion requiring assignation to the subfamily Leptodinioideae. Results either imply polyphyletic origins for the genus *Operculodinium* or that combinations of ventral organization and torsion cannot always be applied rigidly to subdivide the family Gonyaulacaceae.

“The beauty of nature lies in detail; the message, in generality”

Stephen Jay Gould

ACKNOWLEDGMENTS

First and foremost I am grateful to my supervisor, Professor Martin J. Head. His selfless and continuous support was extremely important over the years. I could not imagine having a better supervisor.

Astride Sillis, Howard ("Howie") Melville, and Professor Francine McCarthy are all greatly thanked for their guidance during my first days as a teaching assistant at Brock. They showed me how to treat students with deep respect and appreciation, an invaluable lesson in my life.

My fellow graduate students, Melissa Barnard, Holly Arnold, Heather Racher and Lisa Neville, all made my time in Canada a more fruitful and interesting life experience. I'm particularly grateful to two former graduate students, Eva Fisher and William ("Bill") Gray, who were not only open to different points of view but also shared unforgettable experiences with me during our glamorous life as graduate students.

My deep appreciation also goes to the following: Dr. Carlos Jaramillo and the "Colombian gang" at the Center for Tropical Archaelogy and Palaeoecology (CTPA); Mrs. Camila Vallejo and Mariana Rodríguez, who played a crucial role in the final phase of this thesis; M. Hoppenrath (DZMB, Forschungsinstitut Senckenberg) for making available published and unpublished photomicrographs of *Protoceratium reticulatum*; and K. Mertens (Ghent University) for bringing to attention some of the older literature. K. Matsuoka (Nagasaki University) and K. Mertens provided helpful comments on the episert condition in extant species. The Integrated Ocean Drilling Program provided the samples for this research. Helpful reviews of Chapter 2 of this thesis by L. E. Edwards

and J. Lucas-Clark are greatly appreciated, and especially insightful comments from L. E. Edwards regarding the episert condition.

Brock University, the Smithsonian Tropical Research Institute, AASP–The Palynological Society, and the Geological Society of America all provided financial support at different stages of the research, and they are all thanked. Primary support for the thesis research was provided by a Natural Sciences and Engineering Research Council of Canada Discovery Grant to M. J. Head.

TABLE OF CONTENTS

TABLE OF FIGURES

CHAPTER 1: INTRODUCTION

Extensive research has been conducted on Neogene dinoflagellate cysts (dinocysts) at northern high and middle latitudes (Williams and Bujak, 1977; Piasecki, 1980; Matsuoka, 1983; Bujak, 1984; Mudie, 1987; Head et al., 1989a; Head et al., 1989b; de Vernal and Mudie, 1989; Manum et al., 1989; Mudie, 1989; Versteegh, 1994; Zevenboom, 1995; de Verteuil and Norris, 1996; Poulsen et al., 1996; Louwey et al., 1999; Piasecki, 2003; Munsterman and Brinkhuis, 2004; De Schepper and Head, 2009; Dybkjær and Piasecki, 2010). In contrast, Neogene dinocyst assemblages of the central American Neotropics remain little studied, although an early seminal work by Traverse and Ginsburg (1967) related modern palynomorph distributions to sedimentary environments and hydrological conditions across the top of the modern Great Bahamian Bank (GBB).

Neogene marine palynostratigraphic research in tropical environments of the Americas was pioneered by Wrenn and Kokinos (1986) and Duffield and Stein (1986) who documented well-preserved and richly diverse dinocyst assemblages from the Gulf of Mexico, yet little was discussed regarding their biostratigraphic and ecological implications. Edwards et al. (1998) reported on Neogene dinocysts along with molluscs and isotope geochemistry from southern Florida, confirming a Miocene–Pleistocene age for the Floridian sequences. Head and Westphal (1999) and Westphal et al. (2000) studied palynomorph associations in the Clino Core on the Pliocene and lower Pleistocene slope of the Bahamian Platform, finding that systematic variations in palynomorph assemblages do not track cyclical geochemical trends observed in clay-free

calcareous alternations at the site and thus suggesting a diagenetic origin for such rhythmites. More recent Neogene studies of the tropical Americas include those by Zegarra and Helenes (2011) and Heinrich and Zonneveld (2013), who have used organic-walled and calcareous dinoflagellate cysts, respectively, to relate changes in dinocyst communities to tectonic constriction of the Central American Seaway and hydrological changes triggered by its shoaling and closure.

The present thesis focuses on Ocean Drilling Program (ODP) Site 1007. Located on the modern toe-of-slope of the flat-topped Bahamas Platform, this site provides a relatively complete upper Miocene (23.9 Ma) through lower Pleistocene (1.4 Ma) sedimentary sequence in a highly-resolved temporal network. Although the site was fully studied for its palynological associations (see Appendix 1), this thesis focuses on a distinctive dinocyst, *Operculodinium bahamense* Head *in* Head and Westphal, 1999 which occurs throughout the examined sequence, and which was originally described from nearby lower Pleistocene deposits of the Great Bahamian Bank (Head and Westphal, 1999). This species meets all requirements for assignment to the important cyst-defined genus *Operculodinium* Wall, 1967 emend. Matsuoka et al., 1997, except in possessing very low sutural crests that entirely delineate tabulation on the cyst wall. By comparing the tabulation in *Operculodinium bahamense* with that of the supposedly-related, theca-defined cosmopolitan species *Protoceratium reticulatum* (Claparède and Lachmann, 1859) Bütschli, 1885 – which produces a cyst also assignable to the cyst-defined genus *Operculodinium* – the suprageneric positions of both *Protoceratium* and *Operculodinium* are assessed and their evolutionary implications discussed.

This thesis is based on the recent publication by Paez-Reyes and Head (2013), and as far as possible (without infringing University requirements) follows the style and format of the *Journal of Paleontology* in which it appeared. The following sections of the Introduction provide additional information on Ocean Drilling Program Site1007, a general background on dinoflagellate cyst morphology, and details of the age model developed for the present study. Appendix 1 is a range chart of all species recorded during this study in order to give full palynological context to *Operculodinium bahamense*, as recorded and discussed in this thesis.

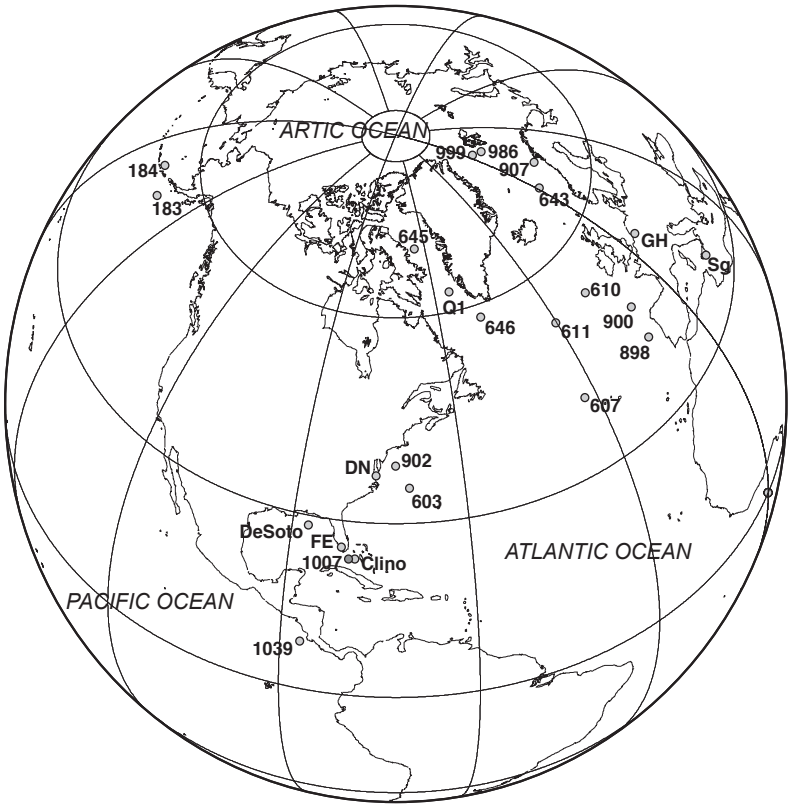

FIGURE 1.1. Location of Ocean Drilling Program Site 1007 and other Neogene localities studied over the last 25 years. Note how poorly studied are tropical areas in the Americas. Abbreviations are: DN=de Verteuil and Norris, 1996; FE=Florida Everglades (Edwards et al., 1998; GH=Groote Heide (Munstermann and Brinkhuis, 2004); Q1=Qulleq-1 well (Piasecki, 2003); and SG=Singa Section (Versteegh, 1994).

OCEAN DRILLING PROGRAM SITE 1007

Ocean Drilling Program Leg 166, Site 1007 (24° 30.254' N, 79° 19.348' W) was drilled in 1996 on the distal slope of the western Great Bahama Bank at a water depth of 647 m (Figure 1.1). A rather complete upper Oligocene to Pleistocene sequence with a total thickness of 1235.5 m was recovered. One of the goals of drilling was to test ideas about how Late Cenozoic sea-level changes might be recorded in the periplatform areas of a carbonate platform (Shipboard Scientific Party, 1997). Seismic and sedimentological studies led to the realization that not only did sea-level changes actively exert control on the stacking pattern and Neogene progradation 25 km westward of the platform edge, but that variations in the intensity of oceanic currents were also responsible for the architectural patterns observed at the toe-of-slope leeward of the Bahamian Platform. Neogene sea-level lowstands generated sequence boundaries across the platform that define genetically related rock packages apparently with chronostratigraphic significance. These sequences are labelled *a* to *q* and their lower sequence boundaries A to Q (Figure 1.2; Anselmetti et al., 2000, Eberli et al., 2002). ODP Site 1007 drilled sequences *c* to *q*. The evolution of sedimentary environments at ODP Site 1007 can be summarized in three main steps:

1) Sequences *q* to *g*: During most of the Early–Late Miocene, sedimentation was concentrated on the slope, with slope sediments consisting of light pelagic wackestones and nannofossil chalks cyclically alternating with dark, neritic wackestones and packstones at meter and centimeter scale. Locally coarse-grained turbidites and slumps are present (Shipboard Scientific Party 1997). The origin of these rhythmic sequences has

been attributed to differential shedding of neritic particles onto a Miocene carbonate ramp. The process hypothetically was driven by sea-level changes in the precession band (Betzler et al., 2000; Reuning et al., 2002). However, the hypothesized differential exporting of aragonitic particles cannot alone explain the couplets, and differential diagenesis is therefore believed to be responsible to some extent for the observed physical contrasts between lithologies (Melim et al. 2002; Reuning et al., 2002).

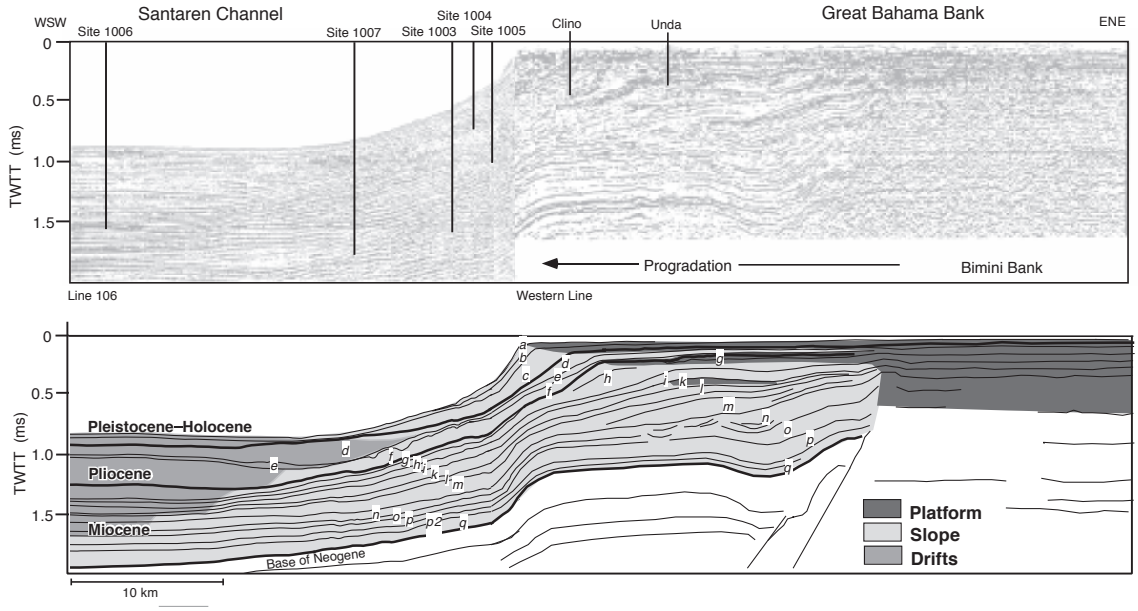

FIGURE 1.2. Seismic profiles 106 and Western Line allow sequence boundaries and sedimentary sequences to be traced across the Great Bahamian Bank and into the basinal areas (see Figure 1.1 for location of seismic lines). Upper figure: Seismic lines showing the location of the remaining five ODP sites drilled in 1996 in close proximity to ODP Site 1007 and the two cores drilled on top of the modern bank as part of the Bahamas Drilling Program (Eberli et al., 1997). Lower figure: Interpreted seismic sequences (lowercase letters *a*–*q*) and sequences boundaries (capital letters A–Q) across the bank and into the Florida Strait. Note how a major transition occurs at the base of sequence *d*. Seismic reflectors below sequence boundary D are mainly chaotic and with little coherence and continuity, whereas above sequence boundary C seismic reflectors in contrast have horizontal continuity. (From Shipboard Scientific Party, 1997).

2) Sequences *f* to *d*: Followed by a rapid sea-level fall in the upper Miocene that produced a disconformity in the lower slope and a hiatus that spans about 3 myr, a rapid rise in sea-level led to a new progradation of the platform edge and turn-on of the carbonate factory exporting sediments towards basinal areas during the upper Miocene–lower Pliocene. With the progradation of the platform edge in the upper Miocene and

lower Pliocene, rhythmic cycles disappear, being replaced by poorly-lithified mudstones, wackstones and nannofossil chalks at the site. Increasing contents of calcareous mud suggest the presence of warmer waters on top of the platform and mainly pelagic sedimentation in basinal areas (Reijmer et al., 2002). Seismic facies show the presence of deep channels downslope that migrate laterally as well as vertically, marking a period of active erosion by submarine channels that, although present in the underlying sequences *q* to *f*, peaked in the lower Pliocene during sequences *f* to *e* (Anselmetti et al., 2000). These channels caused erosion or bypass sedimentation through a slope-parallel depression located at the toe-of-slope (Anselmetti et al., 2000), this process apparently producing a younger hiatus during the lower Pliocene–upper Pliocene as indicated by foraminifer and nannoplankton biostratigraphy (Shipboard Scientific Party, 1997; Wright and Kroon, 2000).

3) Sequence *d* differs from previous sequences in its seismic and sedimentological characteristics. Chaotic reflectors present in the underlying Miocene–lower Pliocene sequences pass uphole into more transparent and horizontally-continuous seismic facies (Anselmetti et al., 2000), this change in seismic properties occurring at the same time as unconsolidated wackstones and nannofossil oozes were being deposited on the slope with very localized dolomitized packstones and wackstones. Peloids of silt and fine-grain size are important rock allochems. Causes for the observed seismic and sedimentological patterns have been attributed to a migration and intensification of oceanic currents eastward of the drift depocenter, which is located in the Miocene–lower Pliocene at ODP Site 1006, 17 km westward of ODP Site 1007 (Anselmetti et al., 2000; Betzler et al., 2000). With the establishment of this depocenter, the slope-parallel depression was filled

in the late Pliocene and Pleistocene with an east or north-dipping contourite system named the Santaren Drift (Anselmetti et al., 2000). The regional intensification of oceanic currents starting at ~3.6 Ma has been extensively documented in the Florida Strait and adjacent areas in the Gulf of Mexico, indicating a cause–effect relationship between intensification of the Florida Current and Loop Current and the final phase in the Closure of the Central American Isthmus (Mullins et al., 1980; Brunner, 1984; Denny et al., 1994; Guertin et al., 2000).

THE DIVISION DINOFLAGELLATA

Dinoflagellates are protists, being single-celled organisms characterized by a life cycle in which an alternation of sexual and asexual phases give rise to schizonts, planozygotes (i.e., motile zygotes) and hypnozygotes (i.e., nonmotile zygotes following a period of sexual reproduction; Evitt, 1985, Figure 1.3). Cysts with ornamented and highly-resistant organic outer walls (dinocysts) are usually assumed to be hypnozygotes, and provide paleontologists with a valuable tool to interpret and infer evolutionary trajectories as well as past ecological and climatic conditions (Sluijs et al., 2005).

Evolutionary relationships in deep time among different groups of dinoflagellates are mainly based on tabulation patterns, a feature unique to dinoflagellates. In the many cases where tabulation on the motile cell is poorly reflected on the cyst surface, suspected relationships cannot be determined. It is therefore important and usually fruitful to determine the tabulation on cysts wherever the opportunity arises. Fensome et al., (1993)

proposed the first comprehensive systematic classification for dinoflagellates using evidence from both fossil and living representatives.

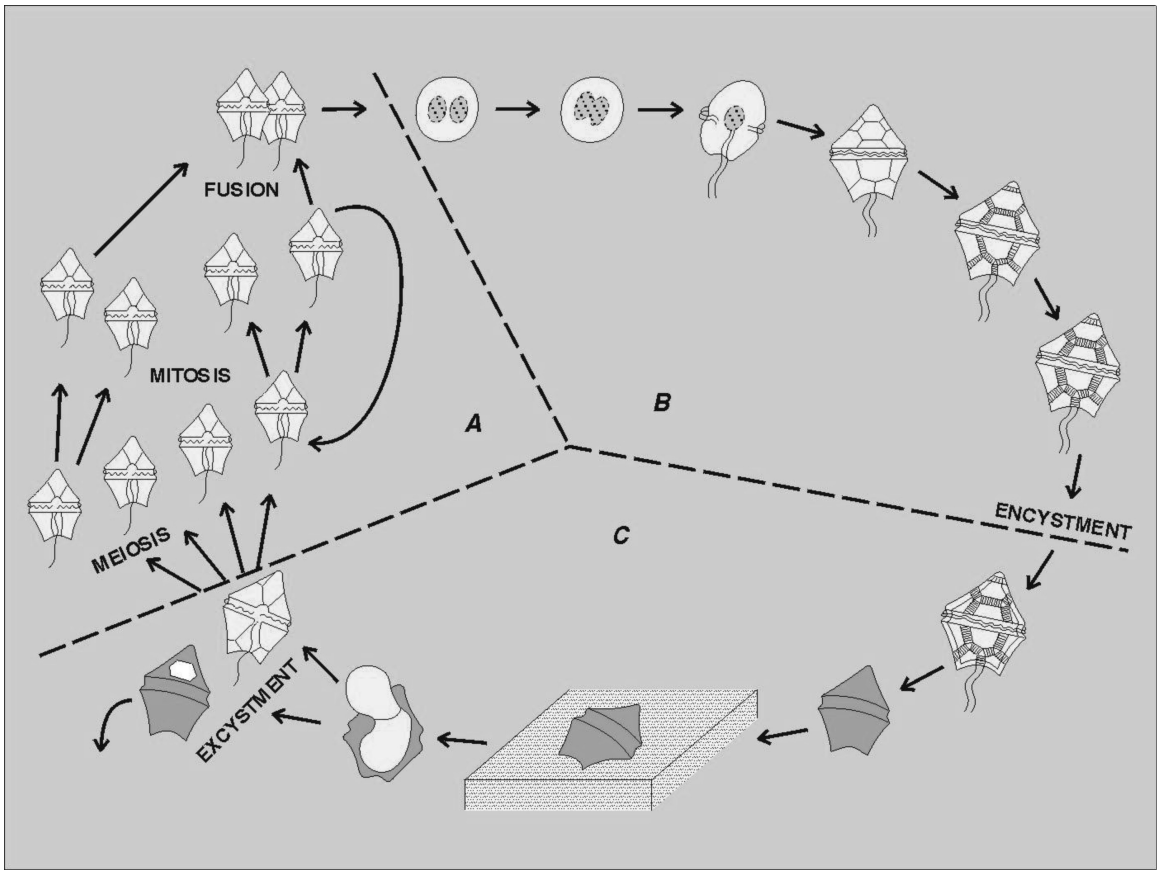

FIGURE 1.3. Idealized life cycle of a dinoflagellate (Evitt, 1985).

The order Gonyaulacales is one of the three most important orders of fossil dinoflagellates. It includes the Gonyaulacaceae, which is one of the most important cyst-producing families in terms of abundance and species diversity in the late Cenozoic and the focus of the present study.

A REVISED AGE MODEL FOR ODP SITE 1007

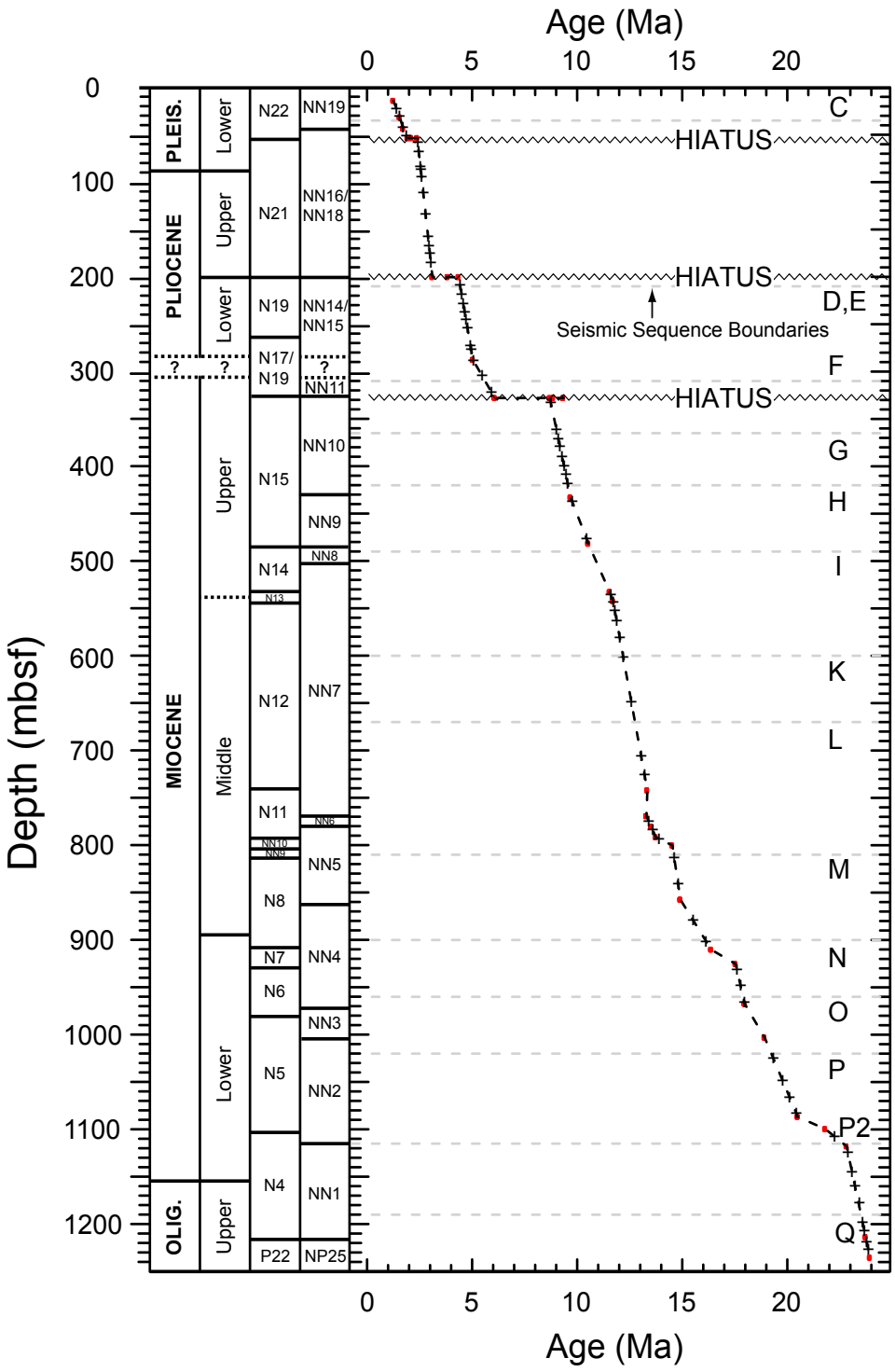

FIGURE 1.4. Age–depth model for ODP Site 1007. Planktonic foraminifera and calcareous nannofossil datums and their depths are from Wright and Kroon (2000) and Shipboard Scientific Party (1997). New geomagnetic and astronomically-tuned ages for each datum are based on Wade et al. (2011) for planktonic foraminifera and Raffi et al. (2006) for calcareous nannofossils.

Event	Nannofossil age (Ma)	Foraminifer age (Ma)	Site 1007 depth (mbsf)
T *Gephyrocapsa* spp. (lg)	1.255		14.23
B *Gephyrocapsa* spp. (lg)	1.560		31.67
B *Gephyrocapsa caribbeanica*	1.720		43.54
T *Globigerinoides extremus*		1.990	53.54
B *Globorotalia truncatulinoides*		1.930	53.54
T*Globorotalia exilis*		2.100	53.54
T *Globorotalia limbata*		2.390	53.54
T *Dentoglobigerina altispira*		3.130	200.34
T *Globorotalia margaritae*		3.840	200.34
T *Globoturborotalia nepenthes*		4.360	200.34
B *Ceratolithus rugosus*	5.054		287.61
B *Globigerinoides conglobatus*		6.080	327.87
B *Globorotalia cibaoensis*		9.340	327.87
B *Globigerinoides extremus*		8.860	327.87
T *Discoaster neohamatus*	8.7		327.99
T *Discoaster hamatus*	9.687		432.99
B *Discoaster hamatus*	10.541		481.68
T *Globorotalia mayeri*		10.530	481.69
B *Globoturborotalia nepenthes*		11.550	532.75
T *Fohsella* spp		11.710	542.48
B *Fohsella fohsi*		13.340	742.12
T *Cyclicargolithus floridanus*	13.294		769.40
T *Sphenolithus heteromorphus*	13.532		780.59
B *Fohsella praefohsi*		13.740	791.54
T *Praeorbulina sicana*		14.530	800.20
B *Orbulina universa**		15.1	808.39
T *Helicosphaera ampliaperta*	14.914		857.50
B *Praeorbulina sicana*		16.380	910.25
T *Catapsydrax dissimilis*		17.540	925.35
T *Sphenolithus belemnos*	17.963		967.44
B *Globigerinatella insueta**		17.690	973.41
B *Sphenolithus belemnos*	18.921		1003.04
B *Globigerinoides altiaperturus*		20.500	1086.75
T "*Paragloborotalia*" *kugleri*		21.810	1099.62
B *Discoaster druggi*	22.824		1117.85
B "*Paragloborotalia*" *kugleri*	23.730		1213.71

FIGURE 1.5. Planktonic foraminifera and nannoplaknton bioevents for the Neogene and Quaternary of ODP Site 1007. Ages are from Wade et al. (2011) for planktonic foraminifera and Raffi et al. (2006) for calcareous nannoplankton. Depths are from Wright and Kroon (2000) and Shipboard Scientific Party. A "*" indicates bioeventes excluded from the calculations.

Ages for samples in this study were interpolated from linear sedimentary rates (Figure 1.3) using "chron", a function for age–depth computation included in PaleoMAS, a package for R (Correa-Metrio et al., 2010). Planktonic foraminifera and calcareous nannofossil datums used for these calculations are presented in Figure 1.4. Depths for the bioevents are from Wright and Kroon (2000) and Shipboard Scientific Party (1997). New geomagnetic and astronomically-tuned ages are given for each datum based on a revised and precise chronology presented in Wade et al. (2011) for planktonic foraminifera and Raffi et al. (2006) for calcareous nannofossils.

PALYNOLOGICAL RESPONSE TO LONG-TERM PALEOECOLOGICAL DYNAMICS IN THE BAHAMAS PLATFORM AND ADJACENT AREAS

Palynological changes in the Bahamas Platform were controlled by at least three factors: 1, paleoceanographic dynamics related to the circulation path established in the middle Miocene between the Loop, Florida and Caribbean currents (Mullin et al., 1987); 2, regional inner dynamics in salinity regimes (Reuning et al., 2006); and 3, short-term sea-level variations (Betzler et al., 2000). Based on variations in palynological assemblages and the groups found using constrained hierarchical cluster analysis (Gordon and Birks, 1972), five intervals from the upper Oligocene through lower Pleistocene can be distinguished at ODP Site 1007 (Figure 1.6). These assemblage zones and their interpretation in strict stratigraphical order are:

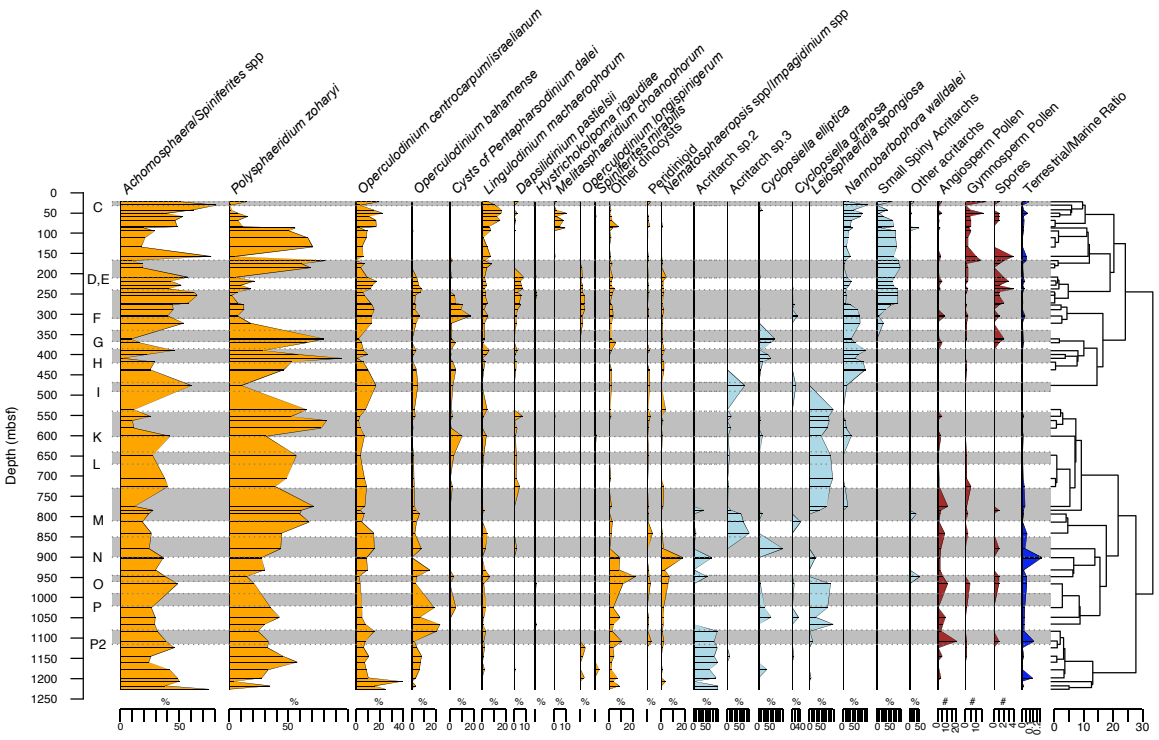

FIGURE 1.6. Constrained hierarchical cluster analysis of selected palynomorphs in the Neogene and Quaternary of ODP Site 1007 (based on data in Appendix 1). Capital letters are sequence boundaries as defined in Eberli et al. (2000). Grey bands correspond to Low-System Tracts and Trangressive System Tracts, while white bands are High System Tracts (sequence stratigraphic framework from Eberli et al., 2000). The percentage of a species refers to the ratio of the number of specimens of certain species to the total number of specimens counted in a slide for that particular group (i.e., dinoflagellate cyst or acritarch).

1) Assemblage zone 1 (1082.80–1226.60 mbsf) is upper Oligocene–lower Miocene and characterized by very low abundances of dinocysts in the lower part, with cysts becoming increasingly more abundant upwards. Within the zone are also common to moderate occurrences of Acritarch sp. 2. The low abundances of dinocysts derived from shallow waters within the lower part of the interval as well as the commonness of acritarchs followed upwards by an increase in the proportion of neritic dinoflagellate cysts, suggest high sea levels and/or a more distant platform edge during the late Oligocene, and a progradation of this edge into the early Miocene (see Betzler et al., 1999). However, progradition was subtle and did not bring vegetation belts close to the site of deposition, as evidenced by the extremely low terrestrial/marine palynomorph

ratios, these being close to zero. Within this interval, as for the rest of Site 1007, *Polysphaeridium zoharyii* and *Achomosphaera*/*Spiniferites* spp. are negatively correlated. This variation, however, shows no systematic changes related to the lower high, low and trangressive system tracts present at ODP Site 1007 (HST, LST and TST respectively; system tracts are from Eberli et al., 1997). Therefore, internal variations within these system tracts perhaps represent only short-term sea-level fluctuations. The dominance of these cysts in addition to *Operculodinium centrocarpum*/*israelianum* and *Operculodinium bahamense* is also evidence of the influence of warm waters atop the Bahamian Platform.

2) Assemblage zone 2 (1082.80–879.10 mbsf) is lower Miocene through middle Miocene. As in the upper part of the immediately underlying sequence, Assemblage zone 2 presents an active input of neritic dinoflagellate cysts with tropical to cosmopolitan affinities, represented by *Achomosphaera*/*Spiniferites* spp., *Dapsilidinium pseudocollerigum*, *Lingulodinium machaerophorum*, *Operculodinium bahamense*, *Operculidinium centrocarpum/israelianum*, and *Polysphaeridium zoharyi*. Acritarchs are also frequent, but in constrast to their high frequencies this group is characterized by very low diversities and dominated particularly by *Leiosphaeridia spongiosa* and locally Acritarch sp. 2. The disappearance of Acritarch sp. 2 corresponds with the upper part of the zone. The negative correlation between *Polysphaeridium zoharyi* and *Spiniferites*/*Achomosphaera* spp., as described in Assemblage zone 1, remains present. However, within this interval there is a subtle coupling between the palynological record and the long-term sequences, and thus *P. zoharyi* is more common within the LST and

early parts of the TST and decreases at the late part of the TST and HST whereas *Achomosphaera*/*Spiniferites* spp has the opposite behaviour.

3) Assemblage zone 3 (879.10–535.80 mbsf) is middle Miocene. *Polysphaeridium zoharyi* and *Spiniferites*/*Achomosphaera* spp. represent on average 70% of the dinocyst assemblages, and *Operculodinium centrocarpum* and *Operculodinium bahamense* show an important decrease in their relative abundances. Acritarchs are common but low in diversity, with *Nannobarbophora walldalei* on the one hand showing low but constant proportions, and *Leiosphaeridia spongiosa* on the other hand exhibiting high relative abundances. The latter species disappears at the top of the zone. Palynological variations correspond with sequence boundaries suggesting that long-term sea-level fluctuations exert an important control on the palynology at Site 1007. Even allowing for the slight decrease in the relative abundances of *Operculodinium centrocarpum* and *Operculodinium bahamense*, the monotonous dinocyst associations suggest very little environmental change.

4) Assemblage zone 4 (535.80-276.98 mbsf) is upper Miocene–lower Pliocene, and defined by an acme of *Nannobarbophora walldalei*, conspicuous increases in foraminiferal linings (not shown in Figure 1.6), and the presence in the lowermost part of the zone of *Achomosphaera/Spiniferites* spp., rare *Operculodinum bahamense*, abundant cysts of *Pentapharsodinium dalei*, and moderate numbers of *O. centrocarpum*/*israelianum,* with *P. zoharyi* varying negatively with *Achomosphaera/Spiniferites* spp. In comparison with the other three zones, Assemblage zone 4 clearly shows that variations in the abundances of species track stratigraphic

sequences. *Polysphaeridium zoharyii* is more common in the LSTs and early TST, and decreases as the sea level rises during the late TSTs and HSTs.

Achomosphaera/*Spiniferites* spp. on the other hand is more common during late parts of the TSTs and HSTs and less abundant during relatively low sea level. An important turnover is recorded in the uppermost part of the zone (above sequence boundary F), given that *Polysphaeridium zoharyi* is for the first time consistently found in low abundances during a LST and TST and *Achomosphaera*/*Spiniferites* spp. is consistently found in high abundances during the late part of the TST and HST. In addition, *L. machaerophorum, Operculodinium*? *longispinigerum, Dapsillidinium pastielsii* and the cysts of *Pentapharsodinium dalei* slightly increases above sequence boundary F. Similar acmes in *Nannobarbophora walldalei* across the Miocene–Pliocene boundary have been reported from Morocco by Warny and Wrenn (1997). This zone appears to reflect a rapid drowning of the platform top, with predominantly normal salinities and warm waters. This event correlates with other floodings at the Miocene/Pliocene boundary and is responsible for the end of the Messinian crisis in the Mediterrean Sea (McKenzie et al., 1999).

5) Assemblage zone 5 (276.98–0 mbsf) is lower Pliocene through upper lower Pleistocene. Two subzones can be recognised within zone 5. The lower subzone spans the lowermost 70 meters of the zone and is represented by variations in the abudances of *Achomosphaera/Spiniferites* spp., *D. pseudocollerigum, L. machaerophorum, N. walldalei, O. bahamense, O. centrocarpum*/*israelianum,* and foraminiferal linings, these taxa decreasing in abundance towards the top of the subzone; whereas *P. zoharyi* becomes increasingly abundant towards the top. The timing of this rise to dominance for

P. zoharyi is truncated by a hiatus of about 2 Ma, this hiatus perhaps caused by intensified bottom currents at ODP Site 1007 and related to a lowstand as recorded on top of the Little Bahamian Bank at 3.4 Ma (Anselmetti et al., 2000; Betzler et al., 2000). The palynological signal indicates a relatively high sea level followed by a lowstand along the Bahamian Platform; in addition this signal may indicate that part of the warm-saline water transported into the Bahamas was the result of increasing tropical waters transported to subtropical latitudes in response to the uplift of the Central American Isthmus. The upper subzone is characterized by common *Achomosphaera/Spiniferites* spp, an important increase in *L. machaerophorum* and *M. choanophorum,* and a decrease in *P. zoharyi*. The increase in *L. machaerophorum* may be related to the important discharges of fresh water and consequent rising nutrient levels that have been reported for Florida at this time.

AIMS OF THIS THESIS

- To document the palynological record and provide a general overview of the upper Oligocene–lower Pleistocene paleoenvironments for subtropical Ocean Drilling Program Site 1007, as a means to providing context for a morphological and taxonomic study of the fossil dinoflagellate cyst *Operculodinium bahamense.*
- To study under light and scanning electron microscopy the tabulation pattern of the fossil dinoflagellate cyst *Operculodinium bahamense* and assess its position at the subfamily level.

- To describe, based on a bibliographic review, the tabulation pattern of the motile stage of the extant dinoflagellate *Protoceratium reticulatum* and asses its position at the subfamily level.
- To explore phylogenetic relationships between the cyst-defined genus *Operculodinium* and the motile-stage-defined genus *Protoceratium*.

CHAPTER 2: THE CENOZOIC GONYAULACACEAN DINOFLAGELLATE GENERA *OPERCULODINIUM* WALL, 1967 AND *PROTOCERATIUM* BERGH, 1881 AND THEIR PHYLOGENETIC RELATIONSHIPS

INTRODUCTION

Little is known of the tabulation pattern in the cyst-defined dinoflagellate genus *Operculodinium* Wall, 1967 emend. Matsuoka et al., 1997 despite its widespread occurrence in Cenozoic deposits and large number of constituent species. A particular hindrance is that *Operculodinium* is restricted to species with a nontabular to intratabular process distribution, and nearly all of the 57 known species of the genus (Fensome et al., 2008; Marret and Kim, 2009) have at most only subtle and incomplete traces of tabulation beyond the possession of a precingular archeopyle (Matsuoka et al., 1997). Moreover, few extant cyst morphotypes attributable to *Operculodinium* have been linked to a motile stage (Head, 1996a). Of these, a morphotype known as *Operculodinium centrocarpum* sensu Wall and Dale (1966) is known to be a cyst of the theca-defined species *Protoceratium reticulatum* (Claparède and Lachmann, 1859) Bütschli, 1885. Fensome et al. (1993, 2008) assigned the genus *Protoceratium* Bergh, 1881 questionably to their new subfamily Cribroperidinioideae (family Gonyaulacaceae, Lindemann 1928), while treating *Operculodinium* as the cyst stage of *Protoceratium*. The assignation was tentative because Fensome et al. (1993) had been unable to find clear illustrations of the dorsal tabulation of *Protoceratium* in the literature, but they noted that the presence of

small first and second postcingular homologs and prominent plate overgrowths are typical of the Cribroperidinioideae. Fensome et al. (2008) explicitly included *Operculodinium* in the Cribroperidinioideae, with *Protoceratium* remaining as a tentative assignation.

The extinct species *Operculodinium bahamense* Head *in* Head and Westphal, 1999 emend., described from the Gelasian (Lower Pleistocene) of the Clino Core, Bahamas (Head and Westphal, 1999; Fig. 2.1), is typical of the genus *Operculodinium* except that its central body bears low sutural ridges that completely express the tabulation except in some details of the sulcus. It is basically similar also to the cyst of the theca-defined species *Protoceratium reticulatum*. Determining the tabulation in both *Operculodinium bahamense* and *Protoceratium reticulatum* therefore promises to elucidate the phylogenetic relationship between *Operculodinium* and *Protoceratium* and reveal whether these genera indeed belong in the subfamily Cribroperidinioideae.

The aims of this study are therefore to describe in detail the tabulation in *Operculodinium bahamense*, re-evaluate and compare the tabulation in *Protoceratium reticulatum*, and assess the suprageneric positions of their respective genera.

MATERIAL

A total of 68 samples from Ocean Drilling Program (ODP) Site 1007, Bahamas Platform (24°30.25'N, 79°19.34'W; Figs. 2.1 and 2.2) were processed for palynology at Brock University, Canada. This site is just 19 km southwest of the Clino Core, which is the type locality of *Operculodinium bahamense*. Samples range from Upper Oligocene

(Chattian) through upper Lower Pleistocene (Calabrian) and consist of gray and white foraminiferal wackestones/packstones, either fully or partially lithified. The lower samples are from ODP Hole 1007C and the upper samples from ODP Hole 1007B (Fig. 2.2). In addition, the palynological slides containing the type material of *Operculodinium bahamense* from the Clino Core, including specimens originally illustrated by Head and Westphal (1999), were reexamined for morphological consistency with specimens from ODP Site 1007.

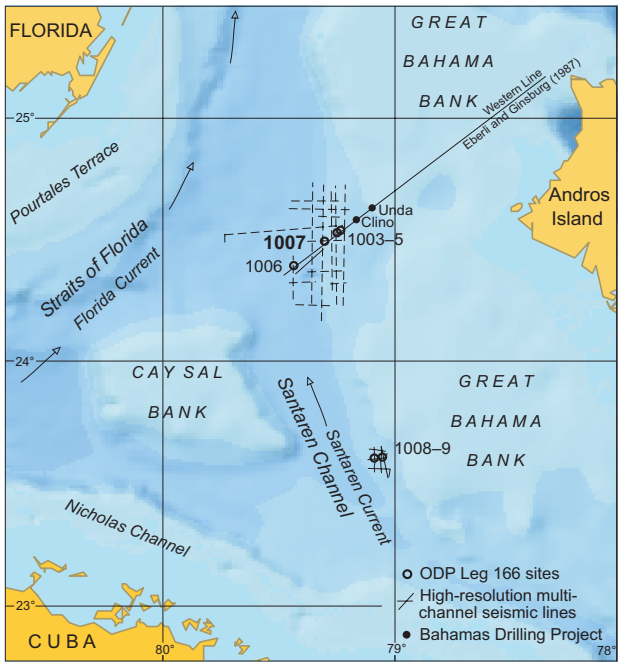

FIGURE 2.1. Location of Ocean Drilling Program (ODP) Site 1007, at the toe-of-slope of the present Bahamian platform margin, along with other ODP Leg 166 sites, seismic sections, and the Clino Core which is the type locality for *Operculodinium bahamense*. Modified from Anselmetti et al. (2000, fig.1).

Protoceratium reticulatum is redescribed and illustrated exclusively from published information (Paulsen, 1907; Lebour, 1925; Woloszynska, 1929; Schiller, 1936 and

ODP Site 1007									Raw Counts		
Series / Subseries		Planktonic foraminiferal zone	Calcareous nannofossil zone	Hole 1007B/C	Sample (core, section, interval in cm)	Depth (meters below sea floor)	Age (Ma)	*O. bahamense* (processes)	*O. bahamense* (no processes)	Total in-situ dinoflagellate cysts
PLEISTOCENE	Lower	N22	NN19	B	3H-3, 045–047	22.45	1.399			264
				B	4H-2, 044–046	30.44	1.538	2	1	351
				B	5H-2, 091–093	42.41	1.705	+	2	321
			NN16–NN18	B	6H-1, 115–116.6	50.65	1.869			305
		N21		B	7H-1, 085–087	58.35	2.414			321
				B	8H-1, 097–099	67.97	2.461	1	1	316
				B	9H-5, 085–086	83.35	2.537		1	321
				B	10H-2, 065–068	86.85	2.554	1		358
PLIOCENE	Upper			B	11X-2, 093–095	94.13	2.590	+	3	308
				B	13X-CC, 025–026	110.85	2.672			311
				B	15X-3, 134–135.5	133.84	2.785	+		311
				B	17X-5, 130.5–132	157.40	2.902	2		323
				B	19X-1, 104–106	167.14	2.949			314
				B	20X-CC, 001–002	175.42	2.990			333
				B	21X-CC, 029–031	184.99	3.037			321
	Lower	N19	NN14–NN15	B	23X-4, 095–096	208.55	4.424	14		354
				B	24X-4, 117–118.5	218.07	4.498	16		326
				B	25X-5, 081–082	228.31	4.578	18	+	338
				B	26X-5, 054–055	237.14	4.647	27	+	349
				B	27X-4, 102–103.5	245.32	4.710	23	+	339
				B	28X-3, 130.5–132	253.41	4.774	9	1	344
		N17–N19		B	30X-3, 144–145	272.14	4.919	8	+	382
				B	31X-1, 008–009	276.98	4.957	13	+	417
?			?	B	32X-2, 068–070	288.19	5.055	9	+	391
MIOCENE	Upper		NN11	B	34X-1, 003–005	304.33	5.472	20		297
				C	3R-1, 060.5–062	321.85	5.924	12		338
		N16	NN10	C	4R-2, 005–007	332.10	8.739	7		309
				C	7R-1, 120–123	360.80	9.008	2		378
				C	8R-1, 129–132	370.59	9.100	+		315
				C	9R-1, 001–004	378.91	9.179	6		219
				C	10R-1,108-113	389.60	9.279	10	1	314
				C	11R-1,130-134	399.40	9.371	6		357
				C	12R-2, 010–015	408.70	9.459	1	1	609
				C	13R-1, 043–046	417.83	9.545	3		297
			NN9	C	15R-1, 043–046	437.13	9.760	13	+	358
				C	19R-1, 070–073	475.90	10.440	7	1	163
		N14	NN8							
		N13	NN7	C	25R-2, 145–150	535.80	11.600	2		91
	Middle	N12		C	26R-1, 071–074.5	543.21	11.716	17		311
				C	27R-1, 031–034	552.41	11.791	9		327
				C	28R-1, 087–090	562.67	11.875	2		327
				C	30R-1, 015–018	581.15	12.026	3		298
				C	32R-1, 073–076	600.93	12.187			269
				C	37R-1, 048–051	648.78	12.578	5		330
				C	43R-1, 012–015	706.12	13.046	4		232
				C	45R-1, 016–019	725.36	13.203	5		242
		N11	NN6	C	50R-1, 124–129	774.50	13.402	7		325
			NN5	C	51R-1, 094–097	783.94	13.596	13		351
		N10		C	52R-3, 132–137	793.24	13.895	20		308
		N9								
		N8		C	54R-2, 000–004	813.30	14.618	14		381
				C	57R-1, 012–015	840.82	14.802	4		162
				C	61R-1, 000–005	879.10	15.514	11		142
	Lower	N7	NN4	C	63R-2, 146–149	901.20	16.128			11
		N6		C	66R-3, 147–152	931.60	17.604	22		181
				C	68R-2, 000–005	948.00	17.773	5		127
				C	70R-1, 014–019	965.80	17.956	9		288
		N5	NN3							
			NN2	C	76R-2, 003–008	1025.00	19.335	11		62
				C	78R-4, 135–140	1048.70	19.782	19		279
				C	80R-4, 000–005	1065.80	20.105	48		251
				C	82R-2, 005–009	1082.80	20.425	32		175
				C	84R-6, 000–005	1107.60	22.254	3		175
				C	86R-3, 136–141	1123.80	22.880	15		373
OLIGOCENE	Upper	N4	NN1	C	88R-5, 000–005	1144.90	23.080	26		337
				C	90R-1, 128–133	1159.70	23.220	25		362
				C	92R-1, 012–017	1177.80	23.391	21		348
				C	94R-2, 000–005	1198.20	23.583	1		29
				C	95R-1, 049–052	1206.99	23.666			38
		P22	NP25	C	96R-3, 009–013	1218.10	23.771	2		80
				C	97R-1, 080–083	1226.60	23.852			10

references therein; Wailes, 1939; Wall and Dale, 1968; Dodge, 1989; Matsuoka, 1990; Hansen et al., 1997; Hoppenrath et al., 2009; Hernández-Becerril et al., 2010; Álvarez et al., 2011; Röder et al., 2012; and as *Gonyaulax grindleyei* in Reinecke, 1967; von Stoch, 1969; Balech, 1988).

METHODS

For each palynological sample, between 3.6 and 27 g of rock were dried overnight at 50°C, weighed and then demineralized in cold hydrochloric and hydrofluoric acids in turn, with distilled water washes in between and afterwards. The organic residues were sieved using a 10-µm Nitex nylon screen, transferred to a 15 ml test tube, and placed in an ultrasound bath for 30 seconds, after which two drops of safranin-o were added. The residues were then sieved again prior to strew mounting on microscope slides using Kaiser's glycerine jelly. Where possible, two slides were made from residue sieved at 10 µm, and one from residue sieved at 20 µm. At least 250 dinoflagellate cysts were counted from the 10 µm slides of each sample where possible, and well-preserved specimens of *Operculodinium bahamense* from the 10 µm and 20 µm slides were selected for detailed morphological analysis. Specimens were observed using light

←

FIGURE *2.2*. Stratigraphic distribution of *Operculodinium bahamense* at ODP Site 1007, showing counts of specimens both with processes and without. The calcareous nannofossil zonation is from the Shipboard Scientific Party (1997), the planktonic foraminiferal zones are from Wright and Kroon (2000), and the series/subseries designations follow Hilgen et al. (2012) except that the Pliocene–Pleistocene boundary follows the international geological time scale (Gibbard and Head, 2010; Gibbard et al., 2010). Boundaries are based on interpolated ages from linear sedimentary plots and age–depth calculations using Wade et al. (2011) for the planktonic foraminiferal datums and Raffi et al. (2006) for the calcareous nannofossils.

microscopy (LM) with a Leica DM 2500 microscope, and photographed using a Leica DMR microscope with Leica DFC 490 camera at Brock University (Figs. 2.3–2.6).

A Zeiss model Evo 40vp scanning electron microscope (SEM) at the Smithsonian Tropical Research Institute, Panama, operating at an acceleration voltage of 8–15 KV, was used to illustrate fine details of the wall surface (Figs. 2.6.7, 2.6.10–2.6.12) and tabulation (Figs. 2.6.8, 2.7) in *Operculodinium bahamense*. Samples were sputter coated with a gold/palladium (60/40) layer no thicker than ca. 50 nm (3 to 4 minutes at 100 μA), using an Anatech Hummer VI-A sputtering system.

The tabulation patterns for both *Operculodinium bahamense* and *Protoceratium reticulatum* were then reconstructed and compared (Figs. 2.8 and 2.9).

The time scale of Hilgen et al. (2012) is used except that the base of the Gelasian Stage, Pleistocene Series, and Quaternary System are all placed at 2.58 Ma, in accordance with the current international geological time scale (Gibbard and Head, 2010; Gibbard et al., 2010).

All specimens illustrated using LM are housed in the Invertebrate Section of the Department of Palaeobiology, Royal Ontario Museum, Toronto, Ontario, Canada, under the catalogue number ROM 53304 for the holotype of *Operculodinium bahamense*, and ROM 62317–62325A and 62325B for the remainder. For each of these specimens, the sample number, microscope slide designation, England Finder reference, and ROM number are given.

MORPHOLOGICAL TERMINOLOGY

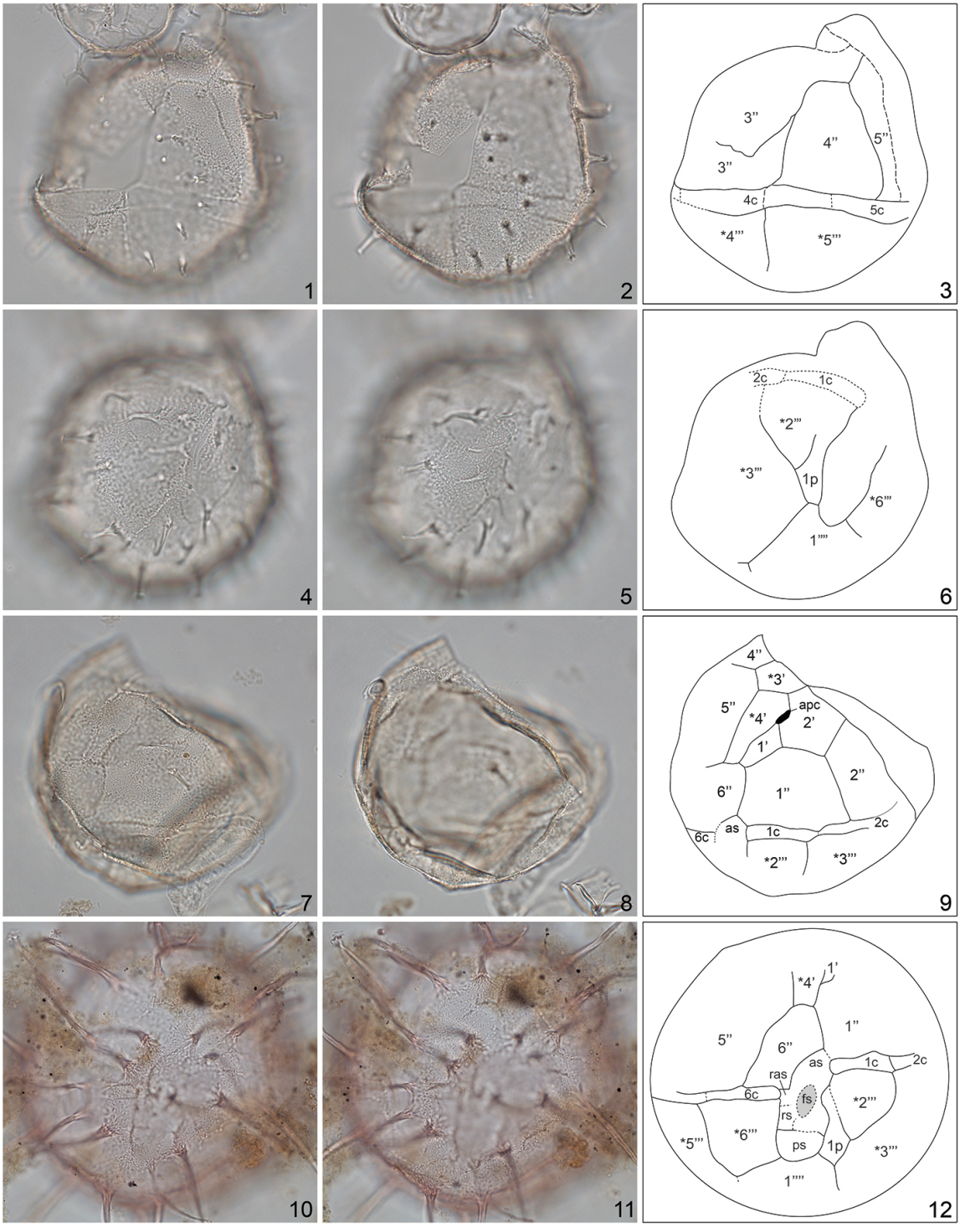
1
2
3
3"
4"
5"
3"
4c
5c
*4'''
*5'''
4
5
6
2c
1c
*2'''
*3'''
1p
*6'''
1''''
7
8
9
4"
*3'
5"
*4'
apc
2'
1'
2"
6"
1"
as
1c
2c
6c
*2'''
*3'''
10
11
12
1'
*4'
1"
5"
6"
as
1c
2c
ras
6c
fs
*2'''
rs
*5'''
*6'''
ps
1p
*3'''
1''''

Labeling of tabulation follows a modified Kofoid system that recognizes homologs (Bujak, 1980, Fensome et al., 1993, 1996; de Verteuil and Norris, 1996).

The new term episert is introduced alongside the existing terms insert, metasert, and exsert to describe the relationship between the first apical plate, or its homolog, and the surrounding plates (Evitt, 1985; Fensome et al., 1993; Fensome et al., 1996; Fig. 2.10). For insert, metasert, and exsert, the first apical plate or its homolog (1' or *1') always contacts the sulcus and may (insert), or may not (metasert, exsert), contact the apical pore complex (Fig. 2.10.1–2.10.3). Episert describes a different episomal tabulation pattern in which the first apical plate (1') contacts the apical pore complex, by definition, but does not contact the sulcus (Fig. 2.10.4–2.10.6). With respect to the episert condition, which is here recognized in *Operculodinium bahamense*, three specific topologies are presently recognized. Episert type I (Fig. 2.10.4) is where 1' is obstructed posteriorly by a contact between the sixth precingular plate or its homolog (6'' or *6'') and the first precingular plate (1''). Episert type II (Fig. 2.10.5) is where both 6'' or *6'' and 4' or *4' contact 1''. Episert type III (Fig. 2.10.6) is where 4' or *4', and possibly Q but not 6'' or *6'', contacts 1''.

←

FIGURE 2.3. Photomicrographs and tracings of *Operculodinium bahamense* Head *in* Head and Westphal, 1999 emend. *1–6*, Holotype. Right latero-dorsal view of *1*, upper surface, *2* slightly lower focus, *4* ventral surface, *5* slightly lower focus, with tracings of *3*, dorsal surface showing archeopyle (3'') and partly broken and overfolded 2'', and *6* ventral surface; note near alignment of *4'''/*5''' with 3''/4'' indicating neutral torsion; central body length, 81 µm; Clino core CUS-K11, slide 3, G18/2; ROM 53433. *7–9*, left latero-apical view of *7* left latero-apical surface, *8* slightly lower focus, and *9* tracing of apical surface showing narrow contact between 1' and 6'' (episert type I), and *3' separated from the apc; central body maximum diameter, 89 µm; Sample 1007C-15R-1, 43–46 cm, slide 20 µm, N47/1; ROM 62317. *10–12*, ventral view of *10* ventral surface, *11* slightly lower focus, and *12* tracing of ventral surface showing details of sulcal tabulation and 1' separated from 6'' (episert type II); central body length, 110 µm; Sample 1007C-3R-1, 60.5–62 cm, slide 2 (10 µm), P53/3; ROM 62318.

SYSTEMATIC PALEONTOLOGY

Abbreviations are as follows: apc=apical pore complex, as=anterior sulcal plate, ras=right accessory sulcal plate, rs=right sulcal plate, ls=left sulcal plate, ps=posterior sulcal plate, fs=flagellar scar.

Division DINOFLAGELLATA (Bütschli, 1885) Fensome et al., 1993

Class DINOPHYCEAE Pascher, 1914

Subclass PERIDINIPHYCIDAE Fensome et al., 1993

Order GONYAULACALES Taylor, 1980

Suborder GONYAULACINEAE (autonym)

Family GONYAULACACEAE Lindemann, 1928

As noted by Fensome et al. (1993), the family Gonyaulacaceae Lindemann, 1928 has the following characteristics: 1) a sexiform hyposomal tabulation pattern, 2) a sulcus more or less midventrally located, 3) an approximately symmetrical antapical outline, 4) absence of strong dorsoventral compression, and 5) six precingular plates. In an attempt to reflect phylogenetic relationships within this family, Fensome et al. (1993) erected three subfamilies, each distinguished by a combination of two features consistently observed through time, namely ventral organization and torsion of the hyposome. The subfamily Leptodinioideae Fensome et al., 1993, whose type genus is *Leptodinium* Klement, 1960, comprises gonyaulacaceans with an L-type ventral organization and sinistral or neutral torsion of the hyposome; the subfamily Criboperidinioideae Fensome et al., 1993, whose type genus is *Cribroperidinium* Neale and Sarjeant, 1962, comprises gonyaulacaceans

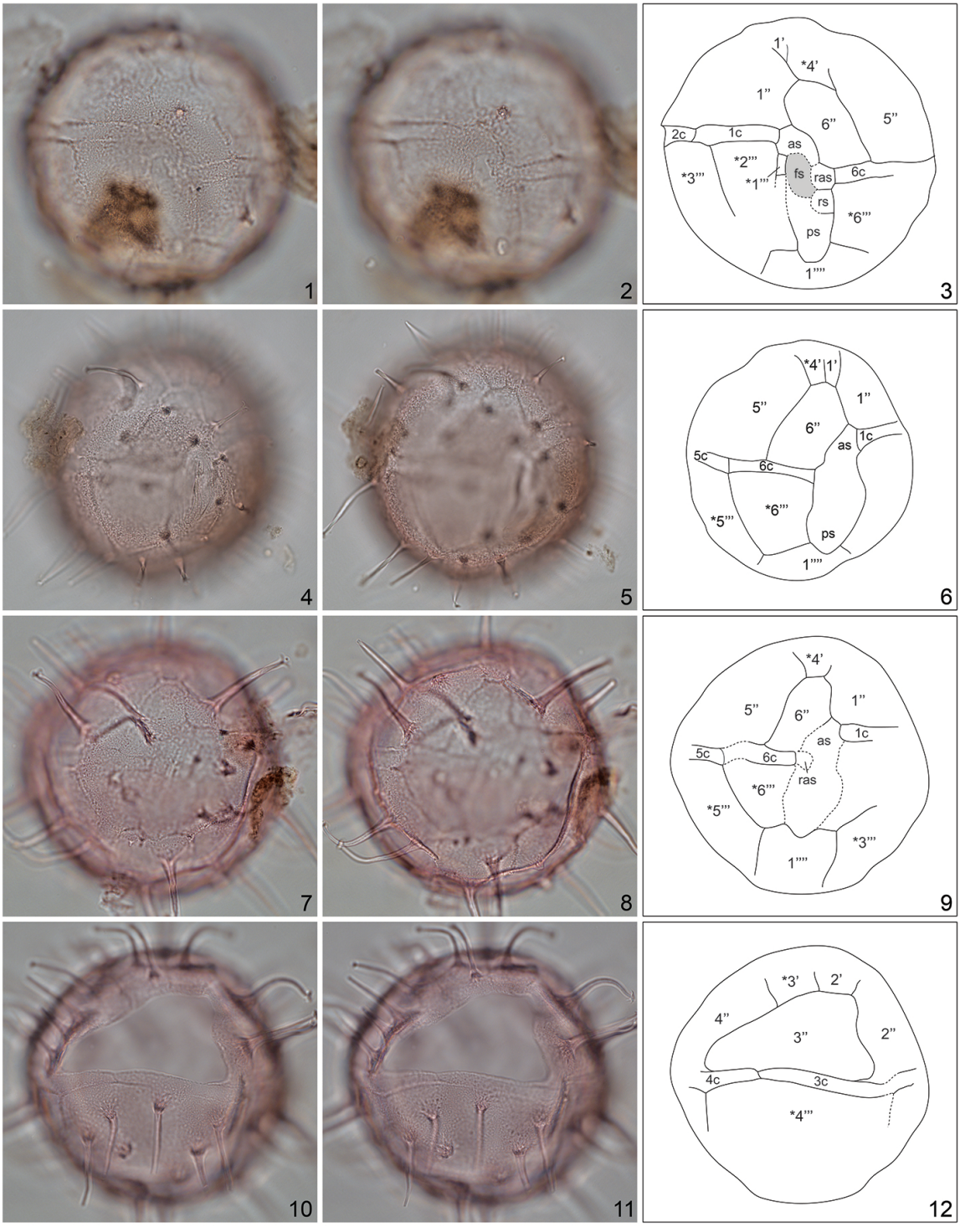
1
2
1'
*4'
1"
6"
5"
2c
1c
as
*2'''
*3'''
*1'''
fs
ras
6c
rs
*6'''
ps
1""
3
4
5
*4'
1'
5"
1"
6"
1c
as
5c
6c
*6'''
*5'''
ps
1""
6
7
8
*4'
5"
6"
1"
1c
as
5c
6c
ras
*6'''
*5'''
*3'''
1""
9
10
11
*3'
2'
4"
3"
2"
4c
3c
*4'''
12

with an L-type ventral organization and dextral torsion of the hyposome; and the subfamily Gonyaulacoideae Fensome et al., 1993, whose type genus is *Gonyaulax* Diesing, 1866, comprises gonyaulacaceans with an S-type ventral organization and neutral torsion of the hyposome (Fensome et al., 1993; Fig. 2.11). Fensome et al. gave an age range of Middle Jurassic through present day for the Criboperidinioideae, Late Jurassic through present day for the Gonyaulacoideae, and Middle Jurassic through Miocene for the Leptodinioideae but noted that some extant species presently assigned to *Gonyaulax* might be leptodinioideans.

Subfamily uncertain

Genus OPERCULODINIUM (Wall, 1967) emend. Matsuoka et al., 1997

Type of genus.—The type of *Operculodinium centrocarpum* (Deflandre and Cookson, 1955) Wall, 1967 emend. Matsuoka et al., 1997.

OPERCULODINIUM BAHAMENSE Head *in* Head and Westphal, 1999 emend.

Figures 2.2–2.7, 2.8.1, 2.9.1–2.9.5, 2.10.4, 2.10.5, 2.12

1989 *Operculodinium* sp. 3; MANUM, BOULTER, GUNNARSDOTTIR, RANGNES, AND SCHOLZE, p. 13, figs. 5, 6.

←

FIGURE 2.4. Photomicrographs and tracings of *Operculodinium bahamense* Head *in* Head and Westphal, 1999 emend. *1–3*, dorsal view of *1* ventral surface, *2* slightly lower focus on sulcus, and *3* tracing of ventral surface showing details of sulcal tabulation and 1' separated from 6'' (episert type II); central body length, 84 µm; Sample 1007C-7R-1, 120–123 cm, slide 2 (10 µm), L57/1; ROM 62319. *4–6*, ventral view of *4* ventral surface, *5* slightly lower focus, and *6* tracing of ventral surface showing narrow contact between 1' and 6'' (episert type I); central body length, 86 µm; Sample 1007C-9R-1, 1–4 cm, slide 1 (10 µm); ROM 62320. *7–12*, ventral view of *7* ventral surface, *8* slightly lower focus, *9* tracing of ventral surface showing *4' but not 1' in contact with 6'' (episert type II), *10* dorsal surface, *11* slightly lower focus, and *12* tracing of dorsal surface showing alignment of *4'''/*5''' with 3''/4'' indicating neutral torsion; central body length, 83 µm; Sample 1007C-10R-1, 108–113 cm, slide 2 (10 µm), O30/1; ROM 62321.

1999 *Operculodinium bahamense* HEAD *IN* HEAD AND WESTPHAL, p. 12, 13, figs. 9.9–9.14, 10.1–10.5.

Original diagnosis.— "A large species of *Operculodinium* with long, sparsely distributed processes; tabulation relatively completely expressed by low sutural ridges that appear as dark narrow lines on surface" (Head *in* Head and Westphal, 1999, p. 13).

Emended diagnosis.—A large species of *Operculodinium* with spherical to subspherical central body whose spongy-fibrous luxuria bears sparsely-distributed, solid to fibrous processes with expanded fibrous bases, terminating distally in minute expansions with aculeate margins. Low sutural ridges demarcate gonyaulacacean, sexiform tabulation with modified L-type ventral organization, neutrally contorted dorsal tabulation, and episert 1'. Plate formula is 2'+*2', 6'', 6c, 5s, *6''', 1p, 1''''. Archeopyle large, angles rounded, formed by loss of third precingular plate; operculum free.

Emended description.—Central body spherical to subspherical, wall consisting of thin, solid pedium, and thicker, distally open, spongy-fibrous luxuria. Surface spongy-fibrous to punctate (Fig. 2.6.7, 2.6.10–2.6.12), may become smoother on sulcus (Fig. 2.6.12). Scattered granules may also occur over surface (Fig. 2.6.8). Processes slender, solid to fibrous, circular in cross-section, with fibrous expanded bases; terminate distally in minute, flared platforms with recurved, aculeate margins, each bearing up to about eight aculeae. Process distribution sparse, apparently intratabular, with the largest plates bearing up to around seven processes (e.g. seven on plate *4''', Fig. 2.5.1, 2.5.2; six on plate 3'', Head and Westphal, 1999, figs. 10.4, 10.5), usually up to four or five processes

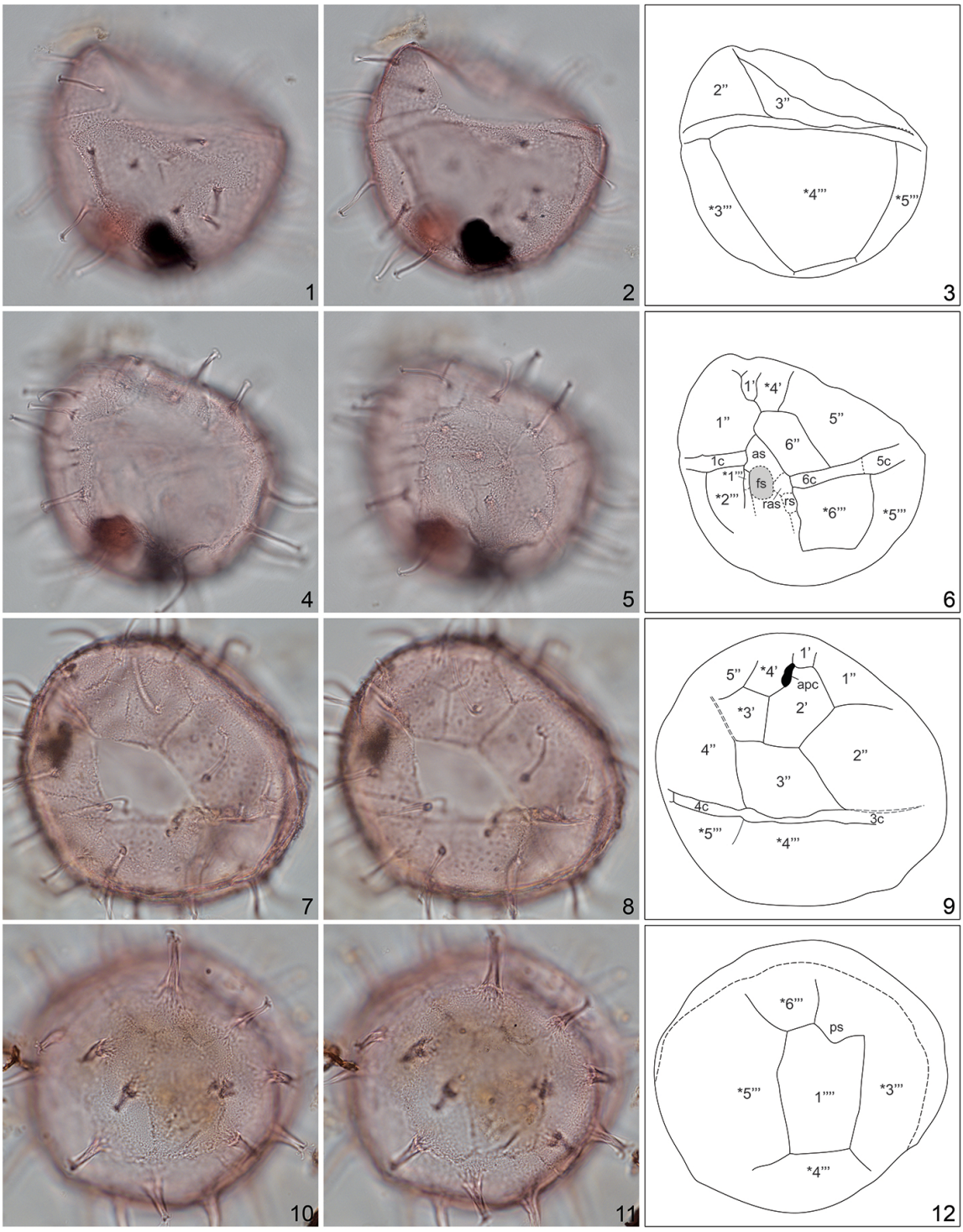
1
2
2”
3”
*4’’’
*3’’’
*5’’’
3
4
5
1’
*4’
1”
5”
6”
as
1c
5c
*1’’’
fs
6c
*2’’’
ras
rs
*6’’’
*5’’’
6
7
8
1’
5”
*4’
apc
1”
*3’
2’
4”
2”
3”
4c
3c
*5’’’
*4’’’
9
10
11
*6’’’
ps
*5’’’
1’’’’
*3’’’
*4’’’
12

on other large plates (e.g. 1'' and *3'''), and usually no more than one on smaller plates (e.g.*2'''). Process bases observed to cross plate boundaries only in the midventral region (Fig. 2.6.8) and occasionally along the cingulum. Process distribution irregular within plate boundaries, adjacent processes may be widely separated or so close as to be fused at base. Processes up to ca. 35 μm long, with length sometimes variable on individual specimens; some specimens devoid of processes (Figs. 2.2, 2.6.1–2.6.6). Shorter, more slender processes may occur in the sulcal area (Fig. 2.6.8). Gonyaulacacean tabulation indicated by low (ca. 1 μm or less) sutural ridges composed of coalesced fibers or granules, appearing under bright field microscopy as dark narrow lines on surface. Apical pore complex (apc) located at anterior pole, slightly left of sulcal midline; individual constituents of apc not distinguishable under light microscopy (Fig. 2.5.7–2.5.9) or SEM (Fig. 2.6.10). Third apical homologue (*3') does not reach apc owing to narrow 2'/*4' contact (Figs. 2.5.7–2.5.9, 2.9.1, 2.9.3–2.9.5). First apical plate (1') either a trapezium reaching 6'' where 1'/6''shorter than 1'/2' (Fig. 2.9.1, 2.9.4) representing episert type I topology (Fig. 2.10.4), or inverted isosceles triangle not reaching 6'' owing to narrow *4'/1'' contact (Fig. 2.9.5) representing episert type II

←

FIGURE 2.5. Photomicrographs and tracings of *Operculodinium bahamense* Head *in* Head and Westphal, 1999 emend. *1–6*, dorsal view of *1* dorsal surface, *2* slightly lower focus, *3* tracing of dorsal surface, *4* ventral surface, *5* slightly lower focus, and *6* tracing of ventral surface showing 1' separated from 6'' (episert type II), and small *1''' separated from 1c; central body length, 90 μm; Sample 1007C-10R-1, 108–113 cm, slide 1 (10 μm), P32/3; ROM 62322. *7–9*, ventral view of *7* dorsal surface, *8* slightly lower focus, and *9* tracing of dorsal surface showing *3' not in contact with the apc; central body maximum diameter, 86 μm; Sample 1007C-54R-2, 0–4 cm, slide 2 (10 μm), J43/0; ROM 62323. *10–12*, antapical view of *10* antapical surface, *11* slightly lower focus, and 12 tracing of antapical surface; central body maximum diameter, 81 μm; Sample 1007B-24X-4, 117–118.5 cm, slide 2 (10 μm), P66/0; ROM 62324.

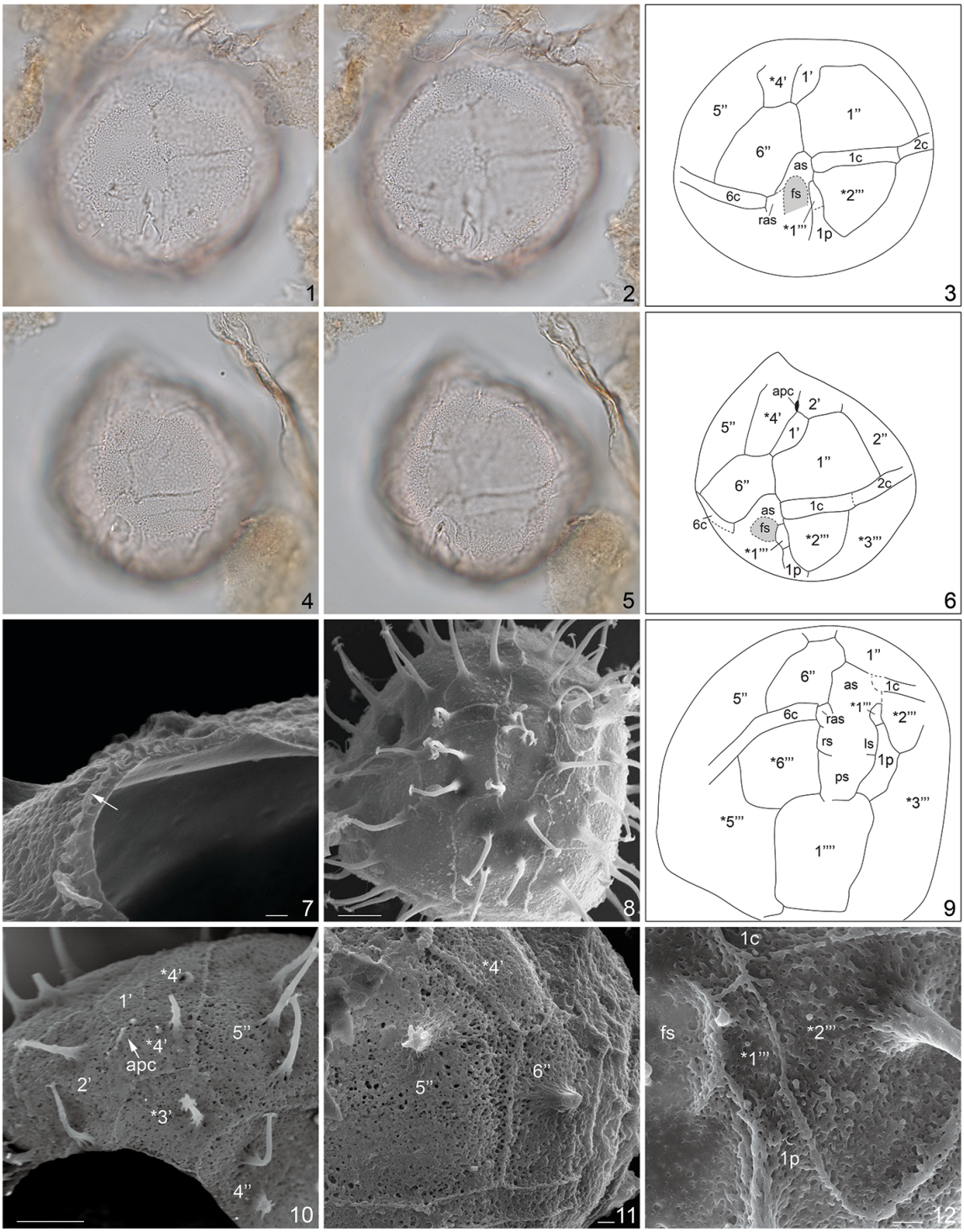
1
2
*4'
1'
5"
1"
6"
2c
1c
as
6c
fs
*2'''
ras
*1'''
1p
3
4
5
apc
2'
*4'
1'
5"
2"
1"
6"
2c
1c
as
6c
fs
*2'''
*3'''
*1'''
1p
6
7
8
1"
6"
as
1c
5"
6c
ras
*1'''
*2'''
rs
ls
*6'''
1p
ps
*3'''
*5'''
1''''
9
*4'
1'
5"
*4'
apc
2'
*3'
4"
10
*4'
5"
6"
11
1c
fs
*2'''
*1'''
1p
12

topology (Fig. 2.10.5). Plate *4' somewhat larger than plate *3'. Plate 3'', lost in archeopyle formation, directly opposite sulcus. Left margin of plate 6'' curves to left, over anterior sulcal plate (as), causing broad 6''/1'' contact. Plate1'' always contacts the anterior sulcal plate. Cingulum narrow, equatorial, descending with displacement of about one width. Sulcus broad, aligned, modified L-type (see Remarks); sulcal plates poorly expressed, but anterior sulcal (as), right accessory sulcal (ras), right sulcal (rs), left sulcal (ls), posterior sulcal (ps) plates may all be partially delineated by faint traces, though not necessarily on every cyst; flagellar scar indicated by elongate indentation left of ras; posterior margin of ps convex where contacting first antapical plate (1''''). First postcingular homolog (*1''') small, does not contact cingulum (Fig. 2.6.12, 2.9.4, 2.9.5); labeled as such because occurs within sulcal area; remaining five plates in series obligatorily labeled postcingular homologs. Neutral torsion on dorsal surface indicated by approximate alignment of *4'''/*5''' with 3''/4'' at cingulum, although *4'''/*5''' typically offset slightly to left of 3''/4'' (as for holotype; Fig. 2.3.1–2.3.3). Boundary

←

FIGURE 2.6. Photomicrographs and tracings of *Operculodinium bahamense* Head *in* Head and Westphal, 1999 emend. *1–6*, LM photos and tracings of specimens without processes. *7–12*, SEM photos and a tracing; scale bar for *7* = 1 µm, for *8* and *10* = 10 µm, for *11* and *12* = 2 µm. *1–3*, ventral view of *1* ventral surface, *2* slightly lower focus, and *3* tracing of ventral surface showing details of sulcus, *1''' separated from 1c, and 1' in narrow contact with 6'' (episert type I); central body length 77 µm; Sample 1007B-31X-1, 8–9 cm, slide 20 µm, H60/4; ROM 62325A. *4–6*, ventral view of *4* ventral surface, *5* slightly lower focus, and *6* tracing of ventral surface showing *1''' separated from 1c, and 1' in narrow contact with 6'' (episert type I); central body length 81 µm; Sample 1007B-31X-1, 8–9 cm, slide 20 µm, T42/0; ROM 62325B. *7*, dorsal view of anterior margin of archeopyle showing sutural crest (arrow) close to margin; Sample 1007C-3R-1, 60.5–62 cm. *8*, *9*, ventral view showing details of ventral tabulation; note in *8*, smaller, more slender processes in sulcal area, and some processes located on plate boundaries, e.g. at *6'''/1''''/ps junction and 5''/6''/6c junction; Sample 1007C-54R-2, 0–4 cm. *10*, dorso-apical view showing anterior margin of archeopyle and apical plates including weakly-expressed apical pore complex (apc); Sample 1007C-10R-1, 108–113 cm. *11*, right-lateral view showing spongy-fibrous luxuria and processes with fibrous bases; Sample 1007C-3R-1, 60.5–62 cm. *12*, ventral view showing spongy-fibrous luxuria, surface becoming punctate to smooth within sulcus; note that *1''' does not quite contact cingulum (an enlargement of specimen in Fig. 7.1); Sample 1007C-3R-1, 60.5–62 cm.

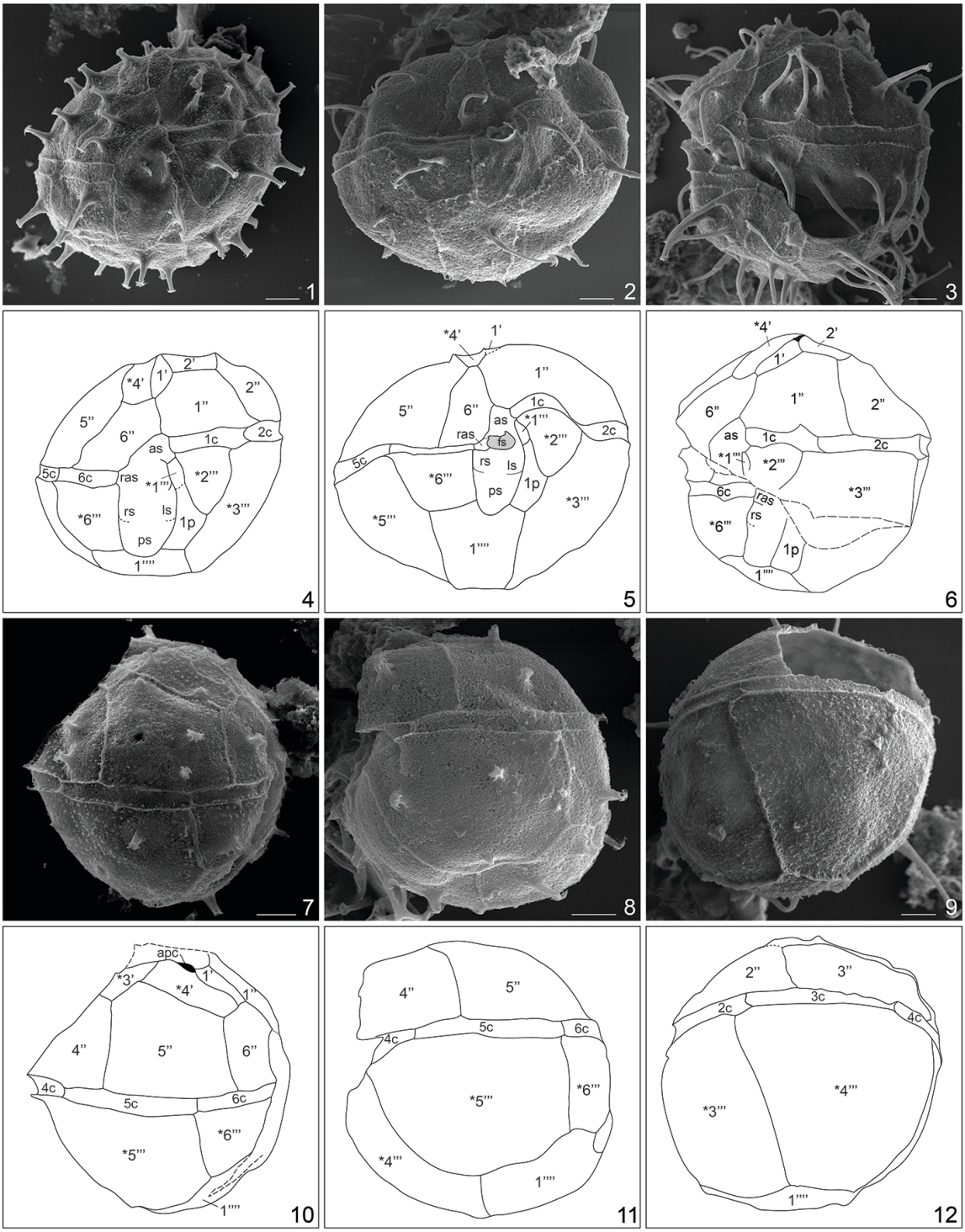
1
2
3
*4'
1'
2'
1''
2''
5''
6''
as
1c
2c
5c
6c
ras
*1'''
*2'''
*6'''
rs
ls
1p
*3'''
ps
1''''
fs
*5'''
4
5
6
7
8
9
apc
*3'
4''
5''
6''
4c
10
11
12
3''
3c
*4'''

*3’’’/*4’’’ offset conspicuously to left of 2’’/3’’ at cingulum (e.g., Fig. 2.5.1–2.5.3). Sexiform hypocystal tabulation; antapical plate (1’’’’) six sided but approximately trapezoidal, widening ventrally; 1’’’’/*6’’’ longer than 1’’’’/1p (Fig. 2.9.2). Archeopyle large, precingular Type 1P (3’’), has rounded angles; low sutural crests, where visible, closely follow entire archeopyle margin including rounded angles (Fig. 2.6.7); operculum free.

Dimensions.—Holotype: central body length, 81 µm; process length, 6–11, µm; wall thickness, ca. 1.7 µm (Head and Westphal, 1999). Upper Pliocene and Lower Pleistocene, Great Bahama Bank: central body maximum diameter, 80(89.7)106 µm; average process length, 7(15.0)24 µm; wall thickness, ca. 0.6(1.1)1.7 µm; 30 specimens measured (Head and Westphal, 1999). ODP Site 1007 (Miocene): central body maximum diameter, 55(84.0)110 µm; average process length, 0(17.2)35.2 µm; wall thickness, ca. 0.5–1.3 µm; 25 specimens measured. ODP Site 1007 (Pliocene): central body maximum diameter, 68(86.1)106 µm; average process length, 0(10.5)31.8 µm; wall thickness, ca. 0.8–3.0 µm; 14 specimens measured. ODP Site 1007 (Pleistocene): central body maximum diameter, 74(84.1)96 µm; average process length, 0(6.0)13.6 µm; wall thickness, ca. 0.8–2.0 µm; seven specimens measured. Overall dimensions: central body maximum diameter, 55(86.1)110 µm; average process length, 0(13.9)35.2 µm; wall

←

FIGURE 2.7. SEM photomicrographs and tracings of *Operculodinium bahamense* Head *in* Head and Westphal, 1999 emend. Scale bars = 10 µm. All specimens are from Sample 1007C-3R-1, 60.5–62 cm, and each photomicrograph represents a different specimen. *1* and *2* are ventral views (see Fig. 6.12 for enlargement), *3* a left lateral view, *7* and *8* are right lateral views, and *9* a left dorso-lateral view. Note in *4*, *6*, and *10* a narrow contact between 1’ and 6’’ (episert type I), and in *5* the absence of such contact (episert type II); and in *4* and *6* the separation of *1’’’ from 1c. Specimen in *9* and *12* shows approximate alignment of *4’’’/*5’’’ with 3’’/4’’ (neutral torsion) and *3’’’/*4’’’ characteristically offset to left of 2’’/3’’.

thickness, ca. 0.5–3.0 µm; 76 specimens measured. See Figure 2.12.

Holotype.—Sample CUS-K 11, slide 3; England Finder reference G18/2. ROM 53304. Clino core, 234.12 m (768.13 ft) below mud pit; Lower Pleistocene (Gelasian),ca. 2.1–2.3 Ma (Head and Westphal, 1999, fig. 9.9–9.12; Fig. 2.3.1–2.3.6).

Type locality.—Clino Core (24°36'07"N, 79°10'41"W), western margin of the Great Bahama Bank (Head and Westphal, 1999).

Comparison.—*Operculodinium giganteum* Wall, 1967, from the Upper Pleistocene and Holocene of the Yucatan Basin, Caribbean, may also have sutural lines, but processes are consistently shorter (2–4 µm) and more densely distributed, and the sulcus is narrow and marked by two parallel rows of spines (Wall, 1967). *Operculodinium wallii* Matsuoka, 1983, from the Upper Miocene–Lower Pleistocene of Japan, lacks sutural lines or ridges. *Operculodinium floridium* Warny and Wrenn, 1997, from the Upper Miocene of Morocco, has shorter (2–10 µm), conical processes whose distribution is dense and distinctly intratabular, and lacks sutural lines or ridges.

Occurrence.—*Operculodinium bahamense* is present from the Chattian (Upper Oligocene) through Calabrian (Lower Pleistocene) at Site 1007, Great Bahama Bank (this study), but its relatively continuous occurrence through the entire studied interval implies that its full stratigraphic range extends above and below the observed occurrence at this site. However, it has a conspicuous highest common occurrence near the Lower/Upper Pliocene boundary. Head and Westphal (1999, but using the current time scale) recorded it from the Zanclean (Lower Pliocene) and Gelasian (lower Lower Pleistocene) of the Clino Core, Great Bahama Bank. It has also been recorded from the upper Middle

Miocene (ODP Hole 642C) and Upper Miocene (ODP Hole 643A) of the Norwegian Sea (as *Operculodinium* sp. 3 in Manum et al., 1989; Bleil, 1989).

Remarks.—The present emendation incorporates new details of the tabulation including the recognition of episert type I and type II topologies (Fig. 2.10.4, 2.10.5),

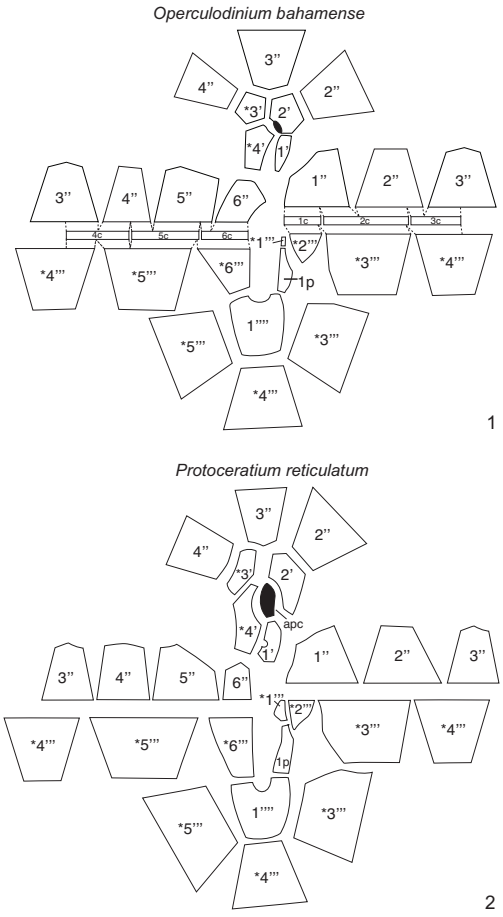

FIGURE 2.8. "Exploded" schematic representation of the tabulation in typical specimens of *1, Operculodinium bahamense* Head *in* Head and Westphal, 1999 emend. (present study), and *2*, *Protoceratium reticulatum* (Claparède and Lachmann, 1859) Bütschli, 1885 (after various sources including von Stosch, 1969; Balech, 1988; and Hansen et al., 1997). All tabulation elements are labeled according to modified Kofoid labelling. Note the overall similarity between these two species, other than the broad contact between 6'' and 1'' in *O. bahamense* and its resulting episert condition for 1'. Sulcal plates are omitted for simplicity.

identification of a modified L-type ventral organization (Fig. 2.9.4, 2.9.5), and neutral torsion on the dorsal surface (Fig. 2.9.3). The last two features require that this species be assigned to the subfamily Leptodinioideae, although such details are unknown for the type species *Operculodinium centrocarpum*, for which reason the genus is not assigned here to a subfamily. It is acknowledged that the ventral organization is not strictly L-type because plate 6'' may not always contact 1' (episert type II topology), and 6'' has an anterior margin that is dithigmate rectilinear at its contact with *4' and 1' (in the case of episert type I topology) rather than the dithigmate geniculate condition that characterizes L-type organization. In other respects, however, the ventral organization has characteristic L-type features including a straight sulcus and a cingulum with ends that are not strongly offset or overhanging (Evitt, 1985, p. 98–100).

The distribution of processes was originally considered nontabular (Head *in* Head and Westphal, 1999) on account of process bases sometimes observed to cross plate boundaries. However, this seems to be restricted to the midventral region and occasionally along the cingulum. Moreover, shorter, more slender processes have been observed in the sulcal area (Fig. 2.6.8), implying that tabulation has some control over process development. Hence, process distribution appears to be intratabular, although the sparse and irregular distribution of processes makes this difficult to confirm. The genus *Operculodinium* includes species with nontabular and intratabular process distributions (Matsuoka et al., 1997).

The emendation also allows for the wide range in process length seen in our ODP Site 1007 material: specimens with longest processes (average process length up to 35.2 μm) occur in the Miocene and Pliocene, those from the Pleistocene typically have much

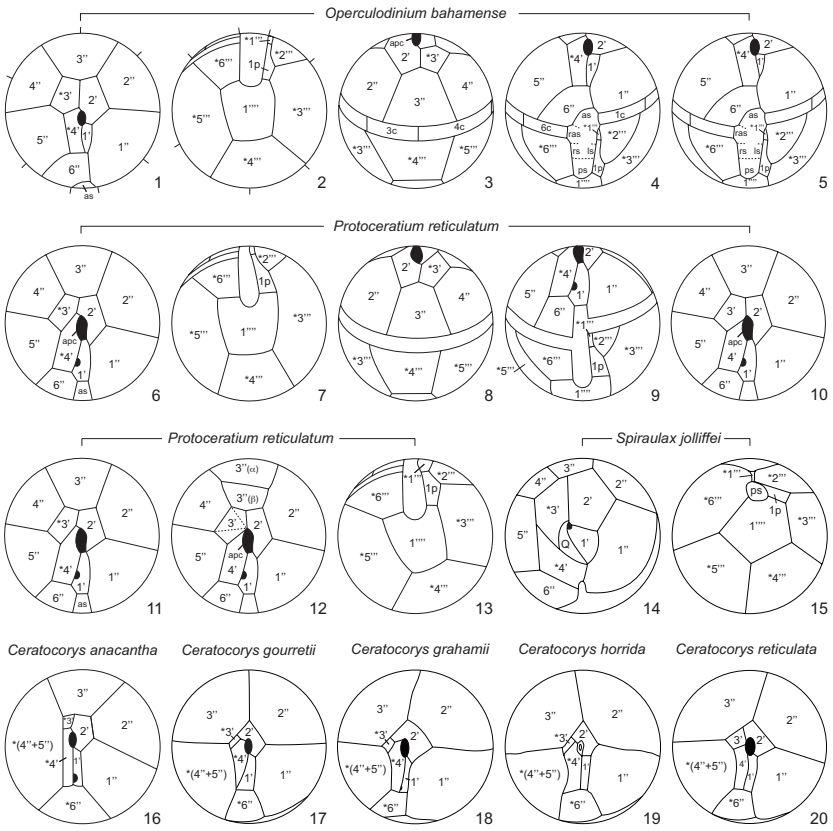

FIGURE 2.9. Tabulation patterns for *Operculodinium bahamense* Head *in* Head and Westphal, 1999 emend., and for the thecae of *Protoceratium reticulatum* (Claparède and Lachmann, 1859) Bütschli, 1885, *Spiraulax jolliffei* (Murray and Whitting, 1899) Kofoid, 1911b, and selected species of the genus *Ceratocorys* Stein, 1883, as projected onto a sphere. *1–5*, *Operculodinium bahamense, 1–4*, in apical, antapical, dorsal and ventral views respectively showing the more usual topology (episert type I) in which 1' narrowly contacts 6''; and *5*, the alternative topology (episert type II) in which 1' does not contact 6''; short bars projecting from the equators in *1* and *2* represent cingular plate boundaries (this study). *6–13*, *Protoceratium reticulatum*, *6–9*, in apical, antapical, dorsal and ventral views respectively showing the typical tabulation pattern in which *3' is an apical homolog as it does not contact the apex, and *8* in this example showing weak dextral torsion (after various sources including von Stosch, 1969; Balech, 1988; and Hansen et al., 1997); *10*, apical view showing the alternative topology in which 3' contacts the apical pore complex, resulting in a true Kofoid third apical plate (adapted from von Stosch, 1969, fig. 7a); *11*, apical view showing 1'' approximately in contact with the apical pore complex (adapted from Balech, 1988, pl. 77, fig. 2); *12*, apical view showing the subdivision of 3' as reported from a cultured cell and indicated by dashed lines (Hansen et al., 1997, fig. 4), and the anomalous division of the third precingular plate (3'') into constituents α and β (adapted from von Stosch, 1969, fig. 7a); and *13*, antapical view in which *4''' has an unusually pronounced offset to the left of the dorsoventral midline, resulting in mild dextral torsion (reconstructed from Reinecke, 1967, fig. 1.D1). *14*, *15*, *Spiraulax jolliffei* showing apical and antapical views respectively, in which *4' broadly contacts 1'', resulting in an episert type III topology (modified from Carbonell-Moore, 1996a, fig. 2a, 2d). *16–20*, selected species of the genus *Ceratocorys* showing contact between *6'' and 1'', resulting in an episert type I topology; *16*, *Ceratocorys anacantha* Carbonell-Moore, 1996b (modified from Carbonell-Moore, 1996b, fig. 1b), *17*, *Ceratocorys gourretii* (modified from Balech, 1988, pl. 80, fig. 5) showing a distinctive topology in which *4' does not contact *6'', *18*, *Ceratocorys grahamii* Carbonell-Moore, 1996b (modified from Graham, 1942, fig. 50B as *Ceratocorys horrida*), *19*, *Ceratocorys horrida* Stein, 1883 (modified from Graham, 1942, fig. 44B, see also Balech, 1988, pl. 79, fig. 4), and *20*, *Ceratocorys reticulata* Graham, 1942 (modified from Graham, 1942, fig. 55B).

shorter processes (average process length no more than 13.6 μm), and specimens almost devoid of processes occur throughout (Figs. 2.2, 2.12). It has not been determined whether shorter processes are linked to reduced paleosalinity, as for the cysts of *Protoceratium reticulatum* (e.g., Head, 2007; Mertens et al., 2011), but this possibility is beinginvestigated. No statistically significant correlation was found between maximum central body diameter and length of processes.

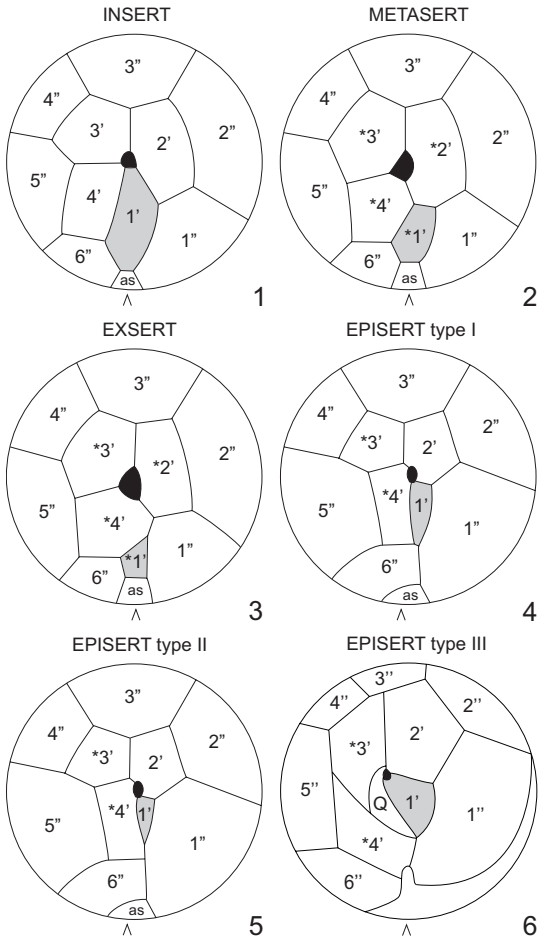

FIGURE 2.10. Variations in relationship of the first apical plate or its homolog (shaded in gray) in the order Gonyaulacales. *1–3* are insert, metasert, and exsert conditions (from Fensome et al., 1996, text-fig. 34); and *4–6* are different types of episert topology in which the first apical plate contacts the apical pore complex but not the sulcus, with *4* and 5 based on *Operculodinium bahamense* Head *in* Head and Westphal, 1999 emend. (present study), and *6* based on *Spiraulax jolliffei* (Murray and Whitting, 1899) Kofoid, 1911b (modified from Carbonell-Moore, 1996a, fig. 2a). The apical pore complex is shown in black, Q is a prepolar plate, and an inverted "v" marks the position of the sulcus.

Subfamily CRIBROPERIDINIOIDEAE Fensome et al., 1993

Genus PROTOCERATIUM Bergh, 1881

Type of genus.—The type of *Protoceratium aceros* Bergh, 1881, this species since considered a taxonomic junior synonym of *Protoceratium reticulatum* (Claparède and Lachmann, 1859) Bütschli, 1885 (Schiller, 1936).

PROTOCERATIUM RETICULATUM (Claparède and Lachmann, 1859) Bütschli, 1885

Figures 2.8.2, 2.9.6–2.9.13

1859 *Peridinium reticulatum* CLAPARÈDE AND LACHMANN, p. 405, pl. 20, fig. 3.

1881 *Protoceratium aceros* BERGH, p. 242, pl. 14, fig. 36.

1885 *Protoceratium reticulatum* (Claparède and Lachmann); BÜTSCHLI, p. 1007, pl. 52, fig. 2.

1936 *Protoceratium reticulatum* (Claparède and Lachmann); SCHILLER, p. 322, 323, fig. 338a–d.

1967 *Gonyaulax grindleyi* REINECKE, p.157–160, pl. 1, fig. 1.

1969 *Gonyaulax grindleyi* Reinecke; VON STOCH, p. 563, figs 6–8.

1982 *Gonyaulax grindleyi* Reinecke; DODGE, p. 210, 211, fig. 25G–I, pl. VIb.

1986 *Gonyaulax grindleyi* Reinecke; HELENES, p.96, 98, text-fig. 14.

1988 *Gonyaulax grindleyi* Reinecke; BALECH, p.169, pl. 77, figs 1–5.

1989 *Protoceratium reticulatum* (Claparède and Lachmann); DODGE, p. 294, fig. 39–42.

1996 *Gonyaulax grindleyi* Reinecke; STEIDINGER AND TANGEN, p. 506–507, pls. 4D, 42.

1997 *Protoceratium reticulatum* (Claparède and Lachmann); HANSEN et al., fig. 2–23.

2009 *Protoceratium reticulatum* (Claparède and Lachmann); HOPPENRATH et al., p. 181–183, fig. k–n.

2011 *Protoceratium reticulatum* (Claparède and Lachmann); ÁLVAREZ et al., fig. 5A–D.

2012 *Protoceratium reticulatum* (Claparède and Lachmann); RÖDER et al., fig. 1a–j.

Description.—Theca polyhedral, slightly longer than broad, epitheca conical, shoulders at boundary of apical/precingular plate series, hypotheca rounded, slightly larger than epitheca. Mature thecae strongly reticulated, usually with one trichocyst pore at centre of each reticulation. Some cells have broad sutural bands ornamented with longitudinal and transverse ridges. Plate formula typically 4' (or 2'+*2'), 6'', 6c, *6''', 1p, 1''''. First apical plate insert, usually with distinct pore on right anterior margin. Fourth apical plate or homolog of significant size (as large or larger than 3'). Sixth precingular plate five-sided with broadly geniculate anterior margin, does not approach a triangular shape, contacts first apical plate. Cingulum slightly anterior to equator, descending with no overhang, displaced ventrally by about one width, with prominent lists. Sulcus straight, reaching almost to antapex. All features of L-type ventral organization consistently present. First postcingular homolog (*1''') small, contained within sulcus. Posterior intercalary plate (1p) long, narrow. Antapical plate (1'''') six-sided, trapezoidal, with distinctive arcuate inset at contact with posterior margin of sulcus; contact with 1p shorter than with 6'''. Sexiform hypothecal tabulation, with

antapical tabulation weakly asymmetrical (e.g., von Stosch, 1969; Fig. 2.9.7) or more strongly asymmetrical (e.g., Reinecke, 1967; Fig. 2.9.13). Plate 3'' relatively small, approximately centered on dorsoventral midline. Hypotheca usually dextrally contorted to varying degrees, with *4'''/*5''' boundary displaced to left of 3''/4'' boundary at cingulum (Fig. 2.9.8). Modified from various sources cited herein.

Cyst has spherical, thin-walled (<1.0 μm) central body, with outer surface bearing scattered granules or columellae, often fine and faintly visible, with interconnecting fibrils sometimes discernible. Processes numerous, nontabular, erect, slender, hollow, circular in cross-section, have smooth surface, may broaden slightly at base, distally open with minute distal expansions. Archeopyle precingular, large with rounded angles, formed by release of 3''; no other indications of tabulation. Central body diameter ca. 33–48 μm; process length up to ca. 14 μm. Based on Rochon et al. (1999, as *Operculodinium centrocarpum* sensu Wall and Dale, 1966).

Holotype.—Claparède and Lachmann (1859, pl. 20, fig. 3, as *Peridinium reticulatum*).

Type locality.—North Sea, collected from modern plankton (Claparède and Lachmann, 1859).

Occurrence.—*Protoceratium reticulatum* is considered a cosmopolitan species and its cysts have a global distribution today (Zonneveld et al., 2013). The cyst has an uncertain stratigraphic range, partly owing to its conflation in the literature with the larger and more robust *Operculodinium centrocarpum* sensu stricto. It extends at least down to the Upper Miocene of Belgium (Louwye and De Schepper, 2010, as *Operculodinium centrocarpum* sensu Wall and Dale, 1966).

Remarks.—Considerable variation exists in the geometry and topology of plates, especially the climactals. The third apical plate may (Wall and Dale, 1968; von Stosch, 1969, fig. 7a; Fig. 2.9.10) or may not (Hansen et al., 1997) contact the apc, and when it does not it has been labeled an anterior intercalary plate (1a; e.g., Dodge, 1989) although we refer to it as the third apical homolog (*3'; Fig. 2.9.6, 2.9.8, 2.9.11). Similarly, the first apical plate may (e.g., von Stosch, 1969; Fig. 2.9.6, 2.9.9, 2.9.10, 2.9.12) or may not (Balech, 1988; Fig. 2.9.11) contact the second apical plate. A ventral pore is usually documented on the right anterior margin of the first apical plate (e.g., Hansen et al., 1997; Fig. 2.9.6, 2.9.9–2.9.12) although it was not recorded either by Reinecke (1967) or Hernández-Becerril et al. (2010). Specimens in culture may display anomalous epithecal tabulation with a subdivided *3' as well as the presence of extra precingular plates (Hansen et al., 1997; Fig. 2.9.12). Plankton from the North Sea have yielded rare exceptions in which plate 3'' is divided into two (Fig. 2.9.12), and the antapical plate similarly divided (von Stosch, 1969).

Torsion in *Protoceratium reticulatum* is often difficult to recognize because of the strong ornament that obscures plate boundaries, and illustrations of the dorsal surface are illusive in the literature (Fensome et al., 1993). However, recent studies by Röder et al. (2012, fig. 1h, 1j) for specimens from the North Sea (the type area for *Protoceratium reticulatum*) and Álvarez et al. (2011, fig. 5A) for specimens from the Pacific off Chile, show pronounced dextral torsion in which the *4'''/*5''' boundary is middorsal. This new evidence, together with L-type ventral organization, small *1''' and *2''', and plate overgrowths (Fensome et al., 1993), allow *Protoceratium reticulatum* to be assigned unequivocally to the Cribroperidinioideae. However, dextral torsion seems to be a

variable feature, as it is weakly expressed judging from reconstructions of the hypotheca (e.g., Wall and Dale, 1968, pl. 3, figs. 7, 8; von Stosch, 1969, fig. 7b), and has even been shown as neutral (Lebour, 1925, pl. 12, fig. 7). Moreover, slight sinistral torsion has been reported by Wailes (1939, fig. 73B, but dextral in fig. 73C) for Pacific specimens off Canada, and Hernández-Becerril et al. (2010) illustrated specimens from the Mexican Pacific that appear slightly sinistrally to neutrally contorted (Hernández-Becerril et al., 2010, figs. 23 and 24 respectively).

TAXONOMIC AND NOMENCLATURAL STATUS OF *PROTOCERATIUM RETICULATUM*

Protoceratium reticulatum was first described, from the North Sea, as *Peridinium reticulatum* by Claparède and Lachmann (1859); and was transferred to the genus *Protoceratium* Bergh, 1881 by Bütschli (1885). It was subsequently accepted that *Protoceratium aceros* Bergh, 1881, described from Danish waters in the Kattegat and serving as the type of the genus *Protoceratium*, was a taxonomic junior synonym of *Protoceratium reticulatum* (Schiller, 1936; Hansen et al., 1997). The type of the genus *Protoceratium* remains the holotype of *Protoceratium aceros* but its correct name is *Protoceratium reticulatum*. The genus *Protoceratium* has itself been considered a junior synonym of *Gonyaulax*, depending upon how broadly authors have treated the circumscription of the latter. Neither original illustrations of *Protoceratium reticulatum* nor *Protoceratium aceros* included analyses of the tabulation, this contributing to

confusion between these two species and with the later *Gonyaulax grindleyi* Reinecke, 1967, described from waters off South Africa (Reinecke, 1967).

Balech (1988) accepted the tabulation formula Po, 0a, 3', 6'', 6c, 6''', 2'''' and 6s for *Protoceratium*, based on the tabulation of *Protoceratium spinulosum* (Murray and Whitting, 1899) Schiller, 1936 (Balech, 1988, pl. 73, figs. 1–4). For the genus *Gonyaulax,* Balech (1988) accepted a tabulation formula Po, 0–3a, 3–4', 6'', 6c, 6''', 2'''' (i.e., 1p and 1'''') and 7–9s, thus distinguishing *Protoceratium* from *Gonyaulax* on a smaller number of sulcal plates.

Dodge's (1989) detailed examination of 20 species ascribed to *Gonyaulax* led him to restrict the tabulation of *Gonyaulax* to Po, 3', 2a, 6'', 6c, 4–8s, 5''', 1p, and 1'''', and resurrect *Protoceratium* with the tabulation Po, 3', 1a, 6'', 6c, s, 6''', 1p, 1''''. The presence of two anterior intercalary plates in *Gonyaulax* and only one in *Protoceratium* served as the most notable difference between these genera. Von Stoch (1969) had earlier recognized that *Protoceratium reticulatum* was synonymous with *Gonyaulax grindleyi* Reinecke 1967, but accepted that it belonged in the genus *Gonyaulax*. As the name *Gonyaulax reticulatum* was preoccupied (by *Gonyaulax reticulatum* Kofoid and Michener, 1911), von Stoch maintained *Gonyaulax grindleyi* as the only acceptable name. Dodge (1989) by resurrecting the genus *Protoceratium* allowed this species to be reunited with its earlier name, as *Protoceratium reticulatum*.

Edwards and Andrle (1992) did not accept Dodge's narrow concept of *Gonyaulax*, and by including forms with 0–3 anterior intercalary plates in this genus, retained the species in *Gonyaulax* as *G. grindleyi*.

Steidinger and Tangen (1996) gave the plate formula for *Gonyaulax* as Po, 3', 2a, 6'', 6c, 7s, 6''', and 2'''' (i.e., 1p and 1''''), and noted that details of the apical pore complex might be used to further separate species or groups within the genus. For *Protoceratium*, Steidinger and Tangen accepted the plate formula Po, 3', 0a, 6'', 6c, 6s, 6''', and 2'''' (i.e., 1p and 1''''). However, they considered *G. grindleyi* not to belong to *Protoceratium* on the assumption that the existing 3' plate is really derived from a 2a intercalary plate, but noted that further interpretation was required. They also observed that the apical pore complex is similar to species of *Alexandrium* and not to *Protoceratium*.

Hansen et al. (1997) conducted a detailed morphological study of *Protoceratium reticulatum* from the southern Kattegat, not far from the type locality of *Protoceratium aceros*. They confirmed that *Protoceratium aceros, Protoceratium reticulatum*, and *Gonyaulax grindleyi* were all synonymous, with the name *Protoceratium reticulatum* taking priority. They described the tabulation as 3', 1a, 6'', 6''', 1p, and 1'''', but noted that nearly 50% of cells analyzed showed contact between 1a and the apc, so that by strict Kofoidian labeling the tabulation would be 4', 0a, 6'', 6''', 1p, and 1'''' for those cells (Fig. 2.9.10). They also noted that for cultured cells, the epithecal tabulation was often anomalous, showing a subdivided 1a plate (i.e. plate 3'; Fig. 2.9.12) and the development of extra precingular plates, as noted above. They cautioned against using tabulation alone to define taxa, and called for cyst type, apc details, plate homology, general cell outline, and cell fine structure all to be used as additional criteria. Hansen et al. (1997) noted that tabulation and fine structure in *Protoceratium reticulatum* indicate a close

relationship to the genus *Gonyaulax*, but they sustained the *Protoceratium* pending further knowledge of fine structural diversity within the genus *Gonyaulax*.

We sustain *Protoceratium* as a genus distinct from *Gonyaulax* on a combination of five lines of evidence. Firstly, the epithecal tabulation appears distinct for *Protoceratium*, based on four climactal plates in *Protoceratium* and five in *Gonyaulax* (Dodge, 1989). Secondly, the ventral organization is of L-type in *Protoceratium reticulatum*, whereas in many species of *Gonyaulax*, including the type species *G. spinifera* (Claparède and Lachmann, 1859) Diesing 1866, it is strongly S-type. Thirdly, the resting cyst of *Protoceratium reticulatum* is characterized by numerous unconnected nontabular processes and an absence of tabulation except for the archeopyle, which is a single precingular plate with rounded angles, and hence assignable to the cyst-defined genus *Operculodinium*; whereas all known resting cysts of the genus *Gonyaulax* (Head, 1996a) either have processes and/or crests that are sutural in distribution (e.g., the cyst-defined genera *Achomosphaera*, *Impagidinium*, *Nematosphaeropsis*, and *Spiniferites*) or lack processes but have precingular archeopyles with well-defined angles (e.g., the cyst-defined genera *Ataxiodinium*, *Bitectatodinium*, and *Tectatodinium*). Fourthly, the apical pore in *Protoceratium* is a narrow slit whereas in *Gonyaulax* it is overlain by a lenticular coverplate (Hansen et al., 1997). Fifthly, molecular studies (e.g., Saldarriaga et al., 2004; Kim et al., 2006; Howard et al., 2009; Riccardi et al., 2009; Kudela et al., 2010) together imply that *Protoceratium reticulatum* is not closely related to species presently analyzed within the genus *Gonyaulax* including the type species *Gonyaulax spinifera*.

The cyst of *Protoceratium reticulatum* was first given a paleontological name by Wall and Dale (1966) who recovered it from the western Atlantic plankton and referred it

to the Miocene species *Operculodinium* (then *Baltisphaeridium*) *centrocarpum* (Deflandre and Cookson, 1955) Wall, 1967. It was subsequently realized that the Miocene species was larger and more robust (Head and Wrenn, 1992; Head, 1996a,b; Matsuoka et al., 1997), and the smaller distinctive Quaternary morphotype was accordingly referred either to "*Operculodinium centrocarpum* sensu Wall and Dale, 1966", or to "the cyst of *Protoceratium reticulatum*". Objection to the latter name was based on the fact that four paleontological species have been linked to *Protoceratium reticulatum*, these being *Operculodinium centrocarpum* sensu Wall and Dale, 1966, *Operculodinium psilatum* Wall, 1967 described from the Holocene of the Caribbean, *Operculodinium israelianum* (Rossignol, 1962) Wall, 1967 described from the Quaternary of the Mediterranean, and *Pyxidinopsis psilata* (Wall and Dale *in* Wall et al., 1973) Head, 1994 described from the Quaternary of the Black Sea; as noted by Head (1996a). However, since *Protoceratium reticulatum* was originally described from the North Sea and is abundant there today, whereas *Operculodinium israelianum* and *Operculodinium psilatum* are not found in modern sediments of the North Sea, it seems highly improbable that either of these cyst types is a cyst of *Protoceratium reticulatum*. *Pyxidinopsis psilata* was recorded by Dale (1996, as *Tectatodinium psilatum*) from the Baltic Sea where *Protoceratium reticulatum* is also found. It now appears that these Baltic Sea cysts are not *Pyxidinopsis psilata* but low-salinity morphotypes of *Protoceratium reticulatum* (Mertens et al., 2011). Accordingly, we consider cysts previously labeled as *Operculodinium centrocarpum* sensu Wall and Dale, 1966 as being unambiguous cysts of *Protoceratium reticulatum*, to which they should now be referred.

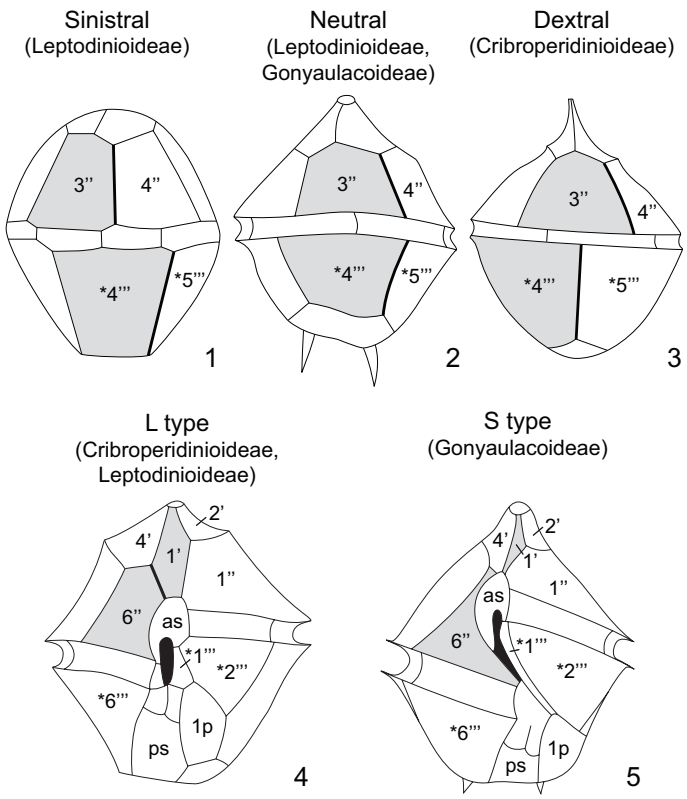

FIGURE 2.11. Dorsal and ventral tabulation arrangements used to divide the Gonyaulacaceae into three subfamilies. *1–3*, dorsal surface showing torsional configurations as exemplified by *1*, *Lithodinia jurassica* (Leptodinioideae); *2*, *Gonyaulax spinifera* (Gonyaulacoideae); and *3*, *Cribroperidinium ventriosum* (Cribroperidinioideae). A heavy line emphasizes the relative positions of the 3''/4'' and *4'''/*5''' boundaries, where 3''/4'' is either shifted to the left (sinistral torsion) or right (dextral torsion), or is aligned (neutral torsion). *4*, *5*, the two main types of ventral organization in the Gonyaulacaceae, *4*, L-type organization as exemplified by *Lingulodinium polyedrum* (Cribroperidinioideae); and *5*, S-type organization as illustrated by *Gonyaulax spinifera* (Gonyaulacoideae) although an overhang at ends of the cingulum is not obligatory for S-type ventral organization (Evitt, 1985, fig. 5.12E–H). However, the quasi-triangular shape of 6'' and lack of contact with 1' are characteristic features of S-type organization. The black area represents the flagellar pore. *Operculodinium bahamense* is herein assigned to the Leptodinioideae (L-type ventral organization, neutral torsion) although it has a modified L-type organization because 6'' always contacts 1'', and 6'' may or may not contact 1'. *Protoceratium reticulatum* is here assigned to the Cribroperidinioideae (L-type ventral organization, dextral torsion). Modified from Fensome et al. (1996, text-figs. 39, 40).

SIGNIFICANCE OF EPISERT CONDITION

The episert condition, here documented in *Operculodinium bahamense* (Leptodinioideae, Gonyaulacaceae), represents an unusual pattern in which the first

apical plate does not contact the sulcus. Two of the three specific episert topologies recognized occur in *Operculodinium bahamense*, these being episert type I (6'' or *6'' contacts 1''; Fig. 2.9.4) and episert type II (6'' or *6'' and 4' or *4'contact 1''; Fig. 2.9.5). The episert condition has also been reported in several extant species. In *Centrodinium mimeticum* (Balech, 1967) Taylor, 1976 (family uncertain, order Gonyaulacales), 6'' narrowly contacts 1'', with 1' tapering to a point just before reaching the sulcus (Balech, 1967, fig. 131, as *Murrayella mimetica*), representing an episert type I topology. A specimen illustrated by Balech (1967, fig. 128) as *Murrayella splendida* also has 1' tapering to a point close to the sulcus and possibly not touching it. A specimen of *Gonyaulax fragilis* (Schütt, 1895) Kofoid, 1911a (Gonyaulacoideae, Gonyaulacaceae) illustrated by Balech (1962, pl. 22, fig. 351) shows 6'' in narrow contact, or possibly not in contact, with 1''. *Spiraulax jolliffei* (Murray and Whitting, 1899) Kofoid, 1911b (Gonyaulacoideae, Gonyaulacaceae) has an extended *4' that broadly contacts 1'' (Kofoid, 1911b; Carbonell-Moore, 1996a; Fig. 2.9.14), representing an episert type III topology.

A characteristic feature of the genus *Ceratocorys* Stein, 1883 (Ceratocoryaceae Lindemann, 1928, Gonyaulacineae) is the broad contact of the sixth precingular homolog (4'' and 5'' are presumed fused, or one is missing) with the first precingular plate, resulting in an episert type I topology (Fig. 2.9.16–2.9.20). Interestingly, molecular data place the type of the genus, *Ceratocorys horrida,* in very close relationship with *Protoceratium reticulatum* (Saldarriaga et al., 2004) indicating that the Ceratocoryaceae, characterized by five precingular plates, L-type ventral organization and strong dextral

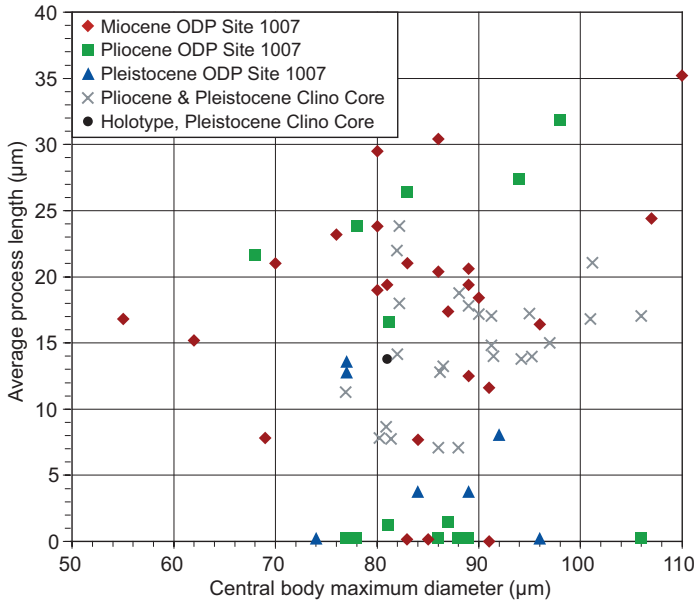

FIGURE 2.12. Measurements for *Operculodinium bahamense* from ODP Site 1007 (this study) and the Clino Core (Head and Westphal, 1999) showing no statistically significant relationship between the maximum central body diameter and average process length.

torsion, is more closely related to the Gonyaulacaceae than previously thought. The episert condition is therefore presently known only in the gonyaulacinean families Ceratocoryaceae and Gonyaulacaceae, both of which appear closely related, although its rarity in the Gonyaulacaceae suggests that it arose independently in these two families.

Species of the genus *Heterodinium* Kofoid, 1906 (Heterodiniaceae Lindemann, 1928) have a small intercalary plate on the midventral epitheca that contacts neither the apex nor sulcus (Fig. 2.13). This plate bears a ventral pore that prompted Fensome et al. (1993) to suggest homology with the first apical plate in other gonyaulacaleans. This would result in yet another kind of relationship, in which the first apical homolog neither contacts the apical pore complex nor the sulcus. However, the ventral pore in gonyaulacaleans is not restricted to the first apical plate, and Dodge (1989) showed

species of the genus *Gonyaulax*, including the type species *Gonyaulax spinifera*, possessing a ventral pore on the anterior margin of the fourth apical homolog (plate 2a of Dodge, 1989). Furthemore, *Heterodinium* species do not have an epithecal tabulation pattern that closely resembles *Operculodinium bahamense*, and molecular evidence suggests that *Heterodinium* is not a gonyaulacalean (Gomez et al., 2012).

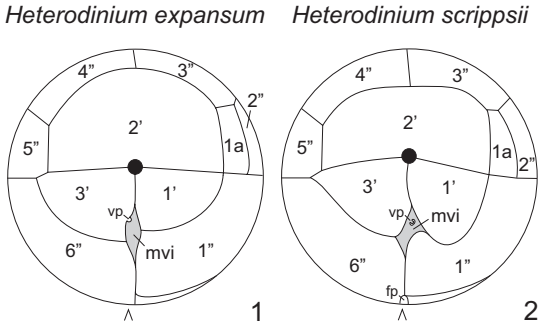

FIGURE 2.13. Epithecal tabulation in two species of the genus *Heterodinium* Kofoid, 1906 showing the midventral intercalary plate (shaded) which has been suggested to be a first apical homolog, although firm evidence is lacking (see text for discussion). *1* based on *Heterodinium expansum* Kofoid 1907 (modified from Kofoid and Adamson, 1933, pl. 5, figs. 5–7), and *2* based on *Heterodinium scrippsii* Kofoid, 1906 (modified from Kofoid and Adamson, 1933, pl. 18, figs. 48–51). The apical pore complex is shown in black, vp=ventral pore, mvi=midventral intercalary plate, fp=flagellar pore, inverted "v"=position of sulcus.

DISCUSSION AND CONCLUSIONS

Reevaluation of the extant, theca-defined species *Protoceratium reticulatum* confirms dextral torsion of the hypotheca and therefore also its placement in the subfamily Cribroperidinioideae, as proposed tentatively by Fensome et al. (1993, 2008). This subfamily therefore contains at least two living species, *Protoceratium reticulatum* and *Lingulodinium polyedrum* (Stein, 1883) Dodge, 1989, in addition to the many fossil genera that extend its history continuously back to the Middle Jurassic (Fensome et al.,

1993). However, along with other aspects of its tabulation, the degree of dextral torsion in *Protoceratium reticulatum* is variable, and specimens with neutral torsion (Lebour, 1925, pl. 12, fig. 7) and even slight sinistral torsion (Hernández-Becerril et al., 2010, fig. 23) have been reported. Whether this results from intraspecific variation or the existence of cryptic species will require closer future attention to the dorsal tabulation (often disregarded by biologists) coupled with molecular analysis. Nonetheless, specimens of *Protoceratium reticulatum* possessing all attributes of the subfamily Cribroperidinioideae have been reported from the North Sea (Röder et al., 2012), which is the type locality of this species. As *Protoceratium reticulatum* is the correct name for the type of the genus, the genus itself must be placed in the Cribroperidinioideae.

Restudy of the cyst-defined *Operculodinium bahamense* reveals a modified L-type ventral organization and neutral torsion, allowing this species to be placed in the subfamily Leptodinioideae. This extends upwards the highest known occurrence of this subfamily from the Miocene (Fensome et al., 1993) to upper Lower Pleistocene (Fig. 2.2). Fensome et al. (1993) noted that some species presently assigned to the extant genus *Gonyaulax* might be leptodinioideans, and our observations reduce this stratigraphic gap.

The assignment of *Operculodinium bahamense* to the Leptodinioideae and *Protoceratium* to the Cribroperidinioideae is paradoxical because the cysts of *Protoceratium reticulatum* are fully circumscribed by the genus *Operculodinium*, suggesting a relationship closer than implied by torsion alone. Moreover, detailed reconstructions of the tabulation in *Operculodinium bahamense* and *Protoceratium reticulatum* reveal strong similarities, even allowing for the episert first apical plate in

Operculodinium bahamense. The sulcal areas are otherwise similar and characteristically L-type in both species, and the apical and antapical tabulation patterns are also similar. These similarities are more striking considering that comparisons of tabulation patterns are being made between thecae and cysts, and that thecamorphic features are not always reflected fully or indeed precisely on the cyst (see Matsuoka et al., 1998, for an extreme example of discordance). Small differences, such as the absence of a pore on the right anterior margin of the first apical plate in *Operculodinium bahamense*, and the isolation of the first postcingular homolog from the cingulum, are therefore not considered overly significant. Accordingly, it is quite unexpected that these two rather similar species should be separated at subfamily level, and implies either that the genus *Operculodinium* is polyphyletic or that the combinations of ventral organization and torsion used to subdivide the family Gonyaulacaceae cannot always be applied rigidly. A combination of both outcomes is in fact possible.

Helenes and Lucas-Clark (1997) and Helenes (2000) have already reported inconsistencies with the criteria used to distinguish subfamilies of the Gonyaulacaceae, and Fensome et al. (1993) themselves noted that these criteria are gradational in nature and in some instances tendencies only. However, with respect to the L-type and S-type tabulation patterns that form the basis of this subfamilial separation, Evitt (1985, p. 102) had remarked that while intermediate patterns do exist, they are fewer in number than those close to the L-type and S-type extremes. Nonetheless, authors continue to document disparities with the subdivision of Fensome et al. (1993). The modern cyst-defined species *Caspidinium rugosum* Marret et al., 2004 and *Pteridocysta cruciformis* Rochon et al., 2002, for example, exhibit a combination of dextral torsion and S-type

ventral organization that hinders assignment at the subfamilial level. *Dimidium* Pearce, 2010, a monospecific genus from the Cretaceous of England, displays a combination of morphologic features characteristic of both the subfamily Leptodinioideae (e.g., L-type ventral organization) and Criboperidiniodeae (e.g., slight dextral organization), further emphasizing the intergradiation of these characters within the family Gonyaulacaceae.

The subfamilial affinity of the genus *Operculodinium* may never be known with certainty because the type species, *Operculodinium centrocarpum* sensu stricto, is extinct and has little reflected tabulation other than the archeopyle. Our results lead us to conclude that it would be premature to assign *Operculodinium* to any of the subfamilies of the Gonyaulacaceae at present, although a thorough revision of the genus is long overdue.

Three additional species could be scrutinized to further our understanding of the genus *Operculodinium*. *Operculodinium israelianum* (Rossignol, 1962) Wall, 1967 is more similar to *Operculodinium centrocarpum* than probably any other species of the genus, and indeed seems to intergrade with it in the Lower Pleistocene (Head, 1996b). It is extant and could therefore be cultured to determine tabulation on the motile cell, and indeed be analyzed directly for molecular phylogeny.

Operculodinium floridium Warny and Wrenn, 1997 is an extinct Miocene–Pliocene species with distinctly intratabular processes that, with careful study, should reveal any dorsal torsion and basic organization of the sulcus. *Operculodinium giganteum* Wall, 1967, from the Upper Pleistocene and Holocene of the Caribbean, might be even more profitable, as sutural lines may be present. Moreover, this species is

possibly extant given its occurrence in Holocene deposits, although we are not aware of reports of living cysts.

Any future revision of the genus *Operculodinium* would need also to consider the large Cretaceous–Miocene genus *Exochosphaeridium* Davey et al., 1966 emend. Helenes, 2000, which differs from *Operculodinium* primarily in the common, but not obligatory, presence of a weakly developed apical horn. However, the one species of *Exochosphaeridium* for which the tabulation has been elucidated, *Exochosphaeridium alisitosense* Helenes, 2000, has an S-type ventral arrangement in contrast to both *Operculodinium bahamense* and *Protoceratium reticulatum*, but dextral torsion in common with *Protoceratium*. Determining such styles of tabulation represents an important challenge in assessing evolutionary relationships between superficially similar species, and in measuring the significance of criteria presently used to subdivide the Gonyaulacaceae.

AFTERWORD

Five palynological assemblage zones that seem to be correlated either to sea-level fluctuations, variations in salinity regimes, and/or changes in oceanic currents can be identified at Ocean Drilling Program (ODP) Site 1007, leeward of the present Bahamas Bank. Although richly diverse and generally well-preserved, Late Cenozoic dinocyst assemblages at this site are dominated almost exclusively by *Polysphaeridium zoharyi* and *Spiniferites*/*Achomosphaera* spp., with *Operculodinium centrocarpum*/*israelianum*, *Operculodinium bahamense*, *Dapsilidinium pastielsii* and *Lingulodinium machaerophorum* as subordinate elements of the assemblages. The persistent presence of *Operculodinium bahamense*, first described from the Plio–Pleistocene of the Clino Core on the western margin of the Great Bahama Bank (Head and Westphal, 1999), has presented an opportunity to study the morphology and taxonomy of this species in detail.

Operculodinium bahamense is of particular interest because, unlike nearly all other species of the important cyst-defined genus *Operculodinium*, it shows traces of tabulation over the entire central body. This feature has allowed the tabulation of Operculodinium bahamense to be elucidated and compared with another dinoflagellate species, the extant *Protoceratium reticulatum*, which produces a cyst that conforms to the genus *Operculodinium*.

Fensome et al. (1993) assigned the genus *Protoceratium*, and by extension *Operculodinium*, questionably to their new subfamily Cribroperidinioideae, but were unable to confirm this assignment owing to a lack of published photographs illustrating

the dorsal surface of *Protoceratium reticulatum*. More recent published and unpublished images of this species have now allowed its morphological and systematic reassessment. Both *Operculodinium bahamense* and *Protoceratium reticulatum* have a sexiform hyposomal tabulation, and L-type (*Protoceratium reticulatum*) or modified L-type (*Operculodinium bahamense*) ventral organization. *Protoceratium reticulatum* has dextral torsion of the hypotheca, confirming assignation of the genus to the subfamily Cribroperidinioideae, whereas *Operculodinium bahamense* has neutral torsion requiring assignation to the subfamily Leptodinioideae. Although such details are known now for *Operculodinium bahamense* they still remain unknown for the type species *Operculodinium centrocarpum* (Deflandre and Cookson, 1955) Wall, 1967, for which reason the genus is not assigned here to a subfamily.

Despite differences in torsion and thus in subfamily assignation, the cysts of *Protoceratium reticulatum* are fully circumscribed by the genus *Operculodinium* suggesting a close relationship contrary to that implied by torsion.

Results on the assignation at the subfamily level of *Protoceratium reticulat*um and *Operculodinium bahamense* imply either polyphyletic origins for the genus *Operculodinium* or that combinations of ventral organization and torsion used to subdivide the family Gonyaulacaceae cannot always be applied rigidly.

REFERENCES

ÁLVAREZ, G., E. URIBE, R. DÍAZ, M. BRAUN, C. MARIÑO, AND J. BLANCO. 2011. Bloom of the Yessotoxin producing dinoflagellate *Protoceratium reticulatum* (Dinophyceae) in Northern Chile. Journal of Sea Research, 65:427–434.

ANSELMETTI, F. S., G. P. EBERLI, AND DING ZAN-DONG. 2000. From the Great Bahama Bank into the Straits of Florida: A margin architecture controlled by sea level fluctuations and ocean currents. Geological Society of America Bulletin, 112:829–844.

BALECH, E. 1962. Tintinnoinea y Dinoflagellata el Pacifico según material de las expediciones Norpac y Downwind del Instituto Scripps de Oceanografía. Revista del Museo Argentino de Ciencias Naturales "Bernardino Rivadavia" e Instituto Nacional de Investigación de las Ciencias Naturales, Zoológicas, 7(1):1–253.

BALECH, E. 1967. Dinoflagelados nuevos o interesantes del Golfo de México y Caribe. Revista del Museo Argentino de Ciencias Naturales "Bernardino Rivadavia" e Instituto Nacional de Investigación de las Ciencias Naturales, Hidrobiología, 2(3):77–126.

BALECH, E. 1988. Los dinoflagelados del Atlántico sudoccidental. Publicaciones Especiales Instituto Español de Oceanografia, 1, 310 p.

BERGH, R. S. 1881. Bidrag til Cilioflagellaternes Naturhistorie. Foreløbige meddelelser. Dansk Naturhistoriskforening I Kjobenhavn, Videnskabelige Meddelelser, Series 4, 3:60–76.

BETZLER, C., J.J.G. REIJMER, K. BERNET, G.P. EBERLI, AND F.S. ANSELMETTI. 1999. Sedimentary patterns and geometries of the Bahamian outer carbonate rampo (Miocene-Lower Pliocene, Great Bahama Bank). Sedimentology, 46:1127–1143.

BETZLER, C., M. PFEIFFER, AND S. SAXENA. 2000. Carbonate shedding and sedimentary cyclicities of a distally steepened carbonte ramp (Miocene, Great Bahama Bank). Geologishe Rundschau–International Journal of Earth Sciences, 89:140–153.

BLEIL, U. 1989. Magnetostratigraphy of Neogene and Quaternary sediment series from the Norwegian Sea: Ocean Drilling Program, Leg 104, p. 829–901. *In* O. Eldholm, J. Thiede, E. Taylor, et al., Proceedings of the Ocean Drilling Program, Scientific Results 104, College Station, Texas.

BRUNNER, C. A. 1984. Evidence for increased volume transport of the Florida Current in the Pliocene and Pleistocene. Marine Geology, 54:223-235.

BUJAK, J. P. 1980. Dinoflagellate cysts and acritarchs from the Eocene Barton Beds of southern England, p. 36–91. *In* J. P. Bujak, C. Downie, G. L. Eaton, and G. L. Williams, Dinoflagellate cysts and acritarchs from the Eocene of southern England. The Palaeontological Association, Special Papers in Palaeontology, 24.

BUJAK, J.P. 1984. Cenozoic dinoflagellate cysts and acritarchs from the Bering Sea and northern North Pacific, DSDP Leg 19. Micropaleontology, 30: 180–212.

BÜTSCHLI, O. 1885. Erster Band. Protozoa, p. 865–1088. *In* Dr. H. G. Bronn's Klassen und Ordnungen des Thier-Reiches, wissenschaftlich dargestellt in Wort und Bild. C. F. Winter'sche Verlagshandlung, Leipzig and Heidelberg.

CARBONELL-MOORE, M. C. 1996a. On *Spiraulax jolliffei* (Murray et Whitting) Kofoid and *Gonyaulax fusiformis* Graham (Dinophyceae). Botanica Marina, 39:347–370.

CARBONELL-MOORE, M. C. 1996b. *Ceratocorys anacantha*, sp. nov., a new member of the family Ceratocoryaceae Lindemann (Dinophyceae). Botanica Marina, 39:1–10.

CLAPARÈDE, É. AND J. LACHMANN. 1859. Études sur les infusoires et les rhizopodes. Institut national génevois, Mémoires, 6 (Mémoire 1):261–482, pl. 14–24. [Imprinted 1858.]

CORREA-METRIO, A., D. H. URREGO, K. R. CABRERA, AND M. B. BUSH. 2012. PaleoMAS: Paleoecological Analysis, R Package Version 2.0-1-The R Project for Statistical Computing.

DALE, B. 1996. Dinoflagellate cyst ecology: modelling and geological applications, p. 1249–1275. *In* J. Jansonius and D. C. McGregor (eds.), Palynology: Principles and Applications. Volume 3. American Association of Stratigraphic Palynologists Foundation, Dallas, Texas.

DAVEY, R. J., C. DOWNIE, W. A. S. SARJEANT, AND G. L. WILLIAMS. 1966. VII. Fossil dinoflagellate cysts attributed to *Baltisphaeridium*. *In* R. J. Davey, C. Downie, W. A. S. Sarjeant, and G. L. Williams, Studies on Mesozoic and Cainozoic dinoflagellate cysts. British Museum (Natural History) Geology, Bulletin, Supplement 3, p. 157–175.

DEFLANDRE, G. AND I. C. COOKSON. 1955. Fossil microplankton from Australian late Mesozoic and Tertiary sediments. Australian Journal of Marine and Freshwater Research, 6:242–313.

DE VERTEUIL, L. AND G. NORRIS. 1996. Miocene dinoflagellate stratigraphy and systematics of Maryland and Virginia. Micropaleontology, 42, supplement, p.1–172.

DIESING, C. M. 1866. Revision der Prothelminthen, Abtheilung: Mastigophoren. Akademie der Wissenschaften zu Wien, Sitzungsberichte, Mathematisch-naturwissenschaftliche Klasse, 52(8):287–401.

DODGE, J. D. 1982. Marine Dinoflagellates of the British Isles. Her Majesty's Stationary Office, London, 303 p.

DODGE, J. D. 1989. Some revisions of the family Gonyaulacaceae (Dinophyceae) based on a scanning electron microscope study. Botanica Marina, 32:275–298.

DE SCHEPPER, S. AND M.J. HEAD. 2009. Pliocene and Pleistocene Dinoflagellate cyst and Acritarch zonation of DSDP Hole 610A, Eastern North Atlantic. Palynology, 33:179-218.

DE VERNAL, A. AND P.J. MUDIE. 1989. Pliocene and Pleistocene palynostratigraphy at ODP sites 646 and 647, eastern and southern Labrador Sea. p. 401-422. *In* S.P. Srivastava, M.A. Arthur, B.M. Clement, A.E. Aksu, J.G. Baldauf, et al., Proceedings of the Ocean Drilling Program, Scientific Results, 105, Ocean Drilling Program, College Station, Texas.

DE VERTEUIL, L. AND G. NORRIS. 1996. Part 1. Dinoflagellate cyst zonation and allostratigraphy of the Chesapeake Group. Micropaleontology, 42, supplement: 1–172.

DENNY III, W. M., J. A. AUSTIN JR, AND R. T. BUFFLER. 1994. Seismic stratigraphy and geologic history of middle Cretaceous through Cenozoic rocks, southern Straits of Florida. AAPG Bulletin, 78: 461–487.

DUFFIELD, S.L. AND J.A. STEIN. 1986. Peridiniacean-dominated dinoflagellate cyst assemblages from the Miocene of the Gulf of Mexico Shelf, Offshore Louisiana.

American Association of Stratigraphic Palynologists Contributions Series, 17: 27–46.

DYBKJÆR, K. AND S. PIASECKI. 2010. Neogene dinocyst zonation for the eastern North Sea Basin, Denmark. Review of Palaeobotany and Palynology, 161:1–29.

EBERLI, G. P. AND R. N. GINSBURG. 1987. Segmentation and coalescence of Cenozoic carbonate platforms, northwestern Great Bahama Bank. Geology, 15:75–79.

EBERLI, G. P., P. K. SWART, D. F. MCNEILL, J. A. M. KENTER, F. S. ANSELMETTI, L. A. MELIM, AND R. N. GINSBURG. 1997. A synopsis of the Bahamas Drilling Project: results from two deep core borings drilled on the Great Bahama Bank. p. 23–41. *In* G. P. Eberli, P. K. Swart, M. J. Malone, et al., Proceedings of the Ocean Drilling Program, Initial Reports, 166, Ocean Drilling Program, College Station, Texas.

EBERLI, G.P., F.S. ANSELMETTI, D. KROON, T. SATO, AND J.M. WRIGHT. 2002. The chronostratigraphic significance of seismic reflectors along the Bahamas Transect. Marine Geology, 185:1–17.

EDWARDS, L. E. AND V. A. S. ANDRLE. 1992. Distribution of selected dinoflagellate cysts in modern marine sediments, p. 259–288. *In* M. J. Head and J. H. Wrenn (eds.), Neogene and Quaternary Dinoflagellate Cysts and Acritarchs. American Association of Stratigraphic Palynologists Foundation, Dallas, Texas.

EDWARDS, L.E., S.D. WEEDMAN, K.R. SIMMONS, T.M. SCOTT, L. BREWSTER-WINGARD, S.E. ISHMAN, N.M. CARLIN. 1998. Litostratigraphy, Petrography, Biostratigraphy, and Strontium-Isotope Stratigraphy of the Surficial Aquifer System of Western Collier County, Florida. US Geological Survey Open-File Report 98-205:1-79.

EVITT, W. R. 1985. Sporopollenin Dinoflagellate Cysts: Their Morphology and Interpretation. American Association of Stratigraphic Palynologists Foundation, Dallas, Texas, p. i–xv, 1–333.

FENSOME, R. A., F. J. R. TAYLOR, G. NORRIS, W. A. S. SARJEANT, D. I. WHARTON, AND G. L. WILLIAMS. 1993. A classification of living and fossil dinoflagellates. Micropaleontology, Special Publication Number 7, 351 p.

FENSOME, R. A., J. B. RIDING, AND F. J. R. TAYLOR. 1996. Dinoflagellates, p. 107–169. *In* J. Jansonius and D. C. McGregor (eds.), Palynology: Principles and Applications. Volume 1. American Association of Stratigraphic Palynologists Foundation, Dallas, Texas.

FENSOME, R. A., R. A. MACRAE, AND G. L. WILLIAMS. 2008. DINOFLAJ2, Version 1. American Association of Stratigraphic Palynologists, Data Series no. 1; http://dinoflaj.smu.ca/wiki/Main_Page

GIBBARD, P. L. AND M. J. HEAD. 2010. The newly-ratified definition of the Quaternary System/Period and redefinition of the Pleistocene Series/Epoch, and comparison of proposals advanced prior to formal ratification. Episodes, 33:152–158.

GIBBARD, P. L., M. J. HEAD, M. J. C. WALKER AND THE SUBCOMMISSION ON QUATERNARY STRATIGRAPHY. 2010. Formal ratification of the Quaternary System/Period and the Pleistocene Series/Epoch with a base at 2.58 Ma. Journal of Quaternary Science, 25:96–102.

GORDON, A.D., AND H.J.B. BIRKS. 1972. Numerical Methods in Quaternary Palaeoecology. I. Zonation of Pollen Diagrams. New Phytologist, 71:961–979.

GRAHAM, H.W. 1942. Studies in the morphology, taxonomy and ecology of the Peridiniales. *In* Scientific Results of Cruise VII of the CARNEGIE during 1928–1929 under command of Captain J.P. Ault. Biology–III. Carnegie Institution of Washington Publication 542, vii+129 p.

GÓMEZ, F., P. LÓPEZ-GARCÍA, J. R. DOLAN, AND D. MOREIRA. 2012. Molecular phylogeny of the marine dinoflagellate genus *Heterodinium* (Dinophyceae). European Journal of Phycology, 47:95–104.

GUERTIN, L. A., T. M. MISSIMER, AND D. F. MCNEILL. 2000. Hiatal duration of correlative sequence boundaries from Oligocene–Pliocene mixed carbonate/siliciclastic sediments of the south Florida Platform. Sedimentary Geology, 134: 1-26.

HANSEN, G., Ø. MOESTRUP, AND K. R. ROBERTS. 1997. Light and electron microscopical observations on *Protoceratium reticulatum* (Dinophyceae). Archiv für Protistenkunde, 147 (1996/97):381–391.

HEAD, M. J. 1994. Morphology and paleoenvironmental significance of the Cenozoic dinoflagellate genera *Tectatodinium* and *Habibacysta*. Micropaleontology, 40:289–321.

HEAD, M. J. 1996a. Chapter 30. Modern dinoflagellate cysts and their biological affinities, p. 1197–1248. *In* J. Jansonius and D. C. McGregor (eds.), Palynology: Principles and Applications. Volume 3. American Association of Stratigraphic Palynologists Foundation, Dallas, Texas.

HEAD, M. J. 1996b. Late Cenozoic dinoflagellates from the Royal Society borehole at Ludham, Norfolk, eastern England. Journal of Paleontology, 70:543–570.

HEAD, M. J. 2007. Last Interglacial (Eemian) hydrographic conditions in the southwestern Baltic Sea based on dinoflagellate cysts from Ristinge Klint, Denmark. Geological Magazine, 144: 987–1013.

HEAD, M.J., G. NORRIS, AND P.J. MUDIE. 1989a. Palynology and dinocyst stratigraphy of the upper Miocene and lowermost Pliocene , ODP Leg 105, Site 646, Labrador Sea. p. 423–451. *In* S.P. Srivastava, M.A. Arthur, B.M. Clement, A.E. Aksu, J.G. Baldauf, et al., Proceedings of the Ocean Drilling Program, Scientific Results, 105, Ocean Drilling Program, College Station, Texas.

HEAD, M.J., G. NORRIS, AND P.J. MUDIE. 1989b. New species of dinocysts and a new species of acritarch from the Upper Miocene and lowermost Pliocene, ODP Leg 105, Site 646, Labrador Sea. p. 453–466. *In* S.P. Srivastava, M.A. Arthur, B.M. Clement, A.E. Aksu, J.G. Baldauf, et al., Proceedings of the Ocean Drilling Program, Scientific Results, 105, Ocean Drilling Program, College Station, Texas.

HEAD, M. J. AND J. H. WRENN (EDS.). 1992. A forum on Neogene–Quaternary dinoflagellate cysts: The edited transcript of a round table discussion held at the Second Workshop on Neogene Dinoflagellates, p. 1–31. *In* M. J. Head and J. H. Wrenn (eds.), Neogene and Quaternary Dinoflagellate Cysts and Acritarchs. American Association of Stratigraphic Palynologists Foundation, Dallas, Texas.

HEAD, M. J. AND H. WESTPHAL. 1999. Palynology and paleoenvironments of a Pliocene carbonate platform: The Clino Core, Bahamas. Journal of Paleontology, 73:1–25.

HEINRICH, S. AND K.A.F. ZOONEVELD. 2013. Influence of the Amazon River development and constriction of the Central American Seaway on Middle/Late Miocene oceanic

conditions at the Ceara Rise. Palaeogeography, Palaeoclimatology, Palaeoecology, 386:599-606.

HELENES, J. 1986. Some variations in the paratabulation of gonyaulacoid dinoflagellates. Palynology, 10:73–110.

HELENES, J. 2000. *Exochosphaeridium alisitosense* n. sp., a new gonyaulacoid dinoflagellate from the Albian of Baja California, Mexico. Micropaleontology, 46:135–142.

HELENES, J., AND J. LUCAS-CLARK. 1997. Morphological variations among species of the fossil dinoflagellate genus *Gonyaulacysta*. Palynology, 21:173–196.

HERNÁNDEZ-BECERRIL, D. U., C. RODRÍGUEZ-PALACIO, AND C. LOZANO-RAMÍREZ. 2010. Morphology of two bloom-forming or potentially toxic marine dinoflagellates from the Mexican Pacific, *Heterocapsa pygmaea* and *Protoceratium reticulatum* (Dinophyceae). Cryptogamie Algologie, 31:245–254.

HILGEN, F. J., L. J. LOURENS, AND J. A. VAN DAM. 2012. The Neogene Period, p. 923–978. *In* F. M. Gradstein, J. G. Ogg, M. D. Schmitz, and G. M. Ogg (eds.), The Geologic Time Scale 2012; volume 2. Elsevier B.V., Amsterdam, The Netherlands.

HOPPENRATH, M., M. ELBRÄCHTER, AND G. DREBES. 2009. Marine Phytoplankton. Selected microphytoplankton species from the North Sea around Helgoland and Sylt. Kleine Senckenberg-Reihe, Band 49, 264 pp.

HOWARD, M. D. A., G. J. SMITH, AND R. M. KUDELA. 2009. Phylogenetic relationships of yessotoxin-producing dinoflagellates based on the large subunit and internal transcribed spacer ribosomal DNA domains. Applied and Environmental Microbiology, 75:54–63.

KIM, K.-Y., Y.-S. KIM, C.-H. HWANG, C.-K. LEE, W.-A. LIM, AND C.-H. KIM. 2006. Phylogenetic analysis of dinoflagellate *Gonyaulax polygramma* Stein responsible for harmful algal blooms based on the partial LSU rDNA sequence data. Algae, 21:283–286.

KLEMENT, K. W. 1960. Dinoflagellaten und Histrichosphaerideen aus dem unteren und mittleren Malm Südwestdeutschlands. Palaeontographica, Abteilung A, 114(1–4):1–104.

KOFOID, C. A. 1906. Dinoflagellata of the San Diego region. – I. On *Heterodinium*, a new genus of the Peridinidae. University of California Publications in Zoology, 2(8):341–368, pl. 17–19.

KOFOID, C. A. 1907. IX. New species of dinoflagellates. Museum of Comparative Zoology at Harvard College, Bulletin, 50:161–207, pl. 1–18.

KOFOID, C. A. 1911a. Dinoflagellata of the San Diego region, IV. The genus *Gonyaulax*, with notes on its skeletal morphology and a discussion of its generic and specific characters. University of California Publications in Zoology, 8(4):187–286, pl. 9–17.

KOFOID, C. A. 1911b. Dinoflagellata of the San Diego region, V. On *Spirulax*, a new genus of the Peridinidae. University of California Publications in Zoology, 8(6):295–300, pl. 19.

KOFOID, C. A. AND A. M. ADAMSON. 1933. The Dinoflagellata: the family Heterodiniidae of the Peridinioidae. Harvard University, Museum of Comparative Zoology, Memoirs, 54(1): 136 p., 22 pl.

KOFOID, C. A. AND J. R. MICHENER. 1911. New genera and species of dinoflagellates. Museum of Comparative Zoology at Harvard College, Bulletin, 54(7):267–302.

KUDELA, R. M., M. D. A. HOWARD, B. D. JENKINS, P. E. MILLER, AND G. J. SMITH. 2010. Using the molecular toolbox to compare harmful algal blooms in upwelling systems. Progress in Oceanography, 85:108–121.

LEBOUR, M. V. 1925. The Dinoflagellates of Northern Seas. Marine Biological Association of the United Kingdom, Plymouth, p. i–vi, 1–250.

LINDEMANN, E. 1928. Abteilung Peridineae (Dinoflagellatae), p. 3–104. *In* A. Engler and K. Prantl (eds.), Die Natürlichen Pflanzenfamilien nebst ihren Gattungen und wichtigeren Arten insbesondere den Nutzpflanzen. Zweite stark vermehrte und verbesserte Auflage herausgegeben von A. Engler. 2 Band. Wilhelm Engelmann, Leipzig.

LOUWYE, S. AND S. DE SCHEPPER. 2010. The Miocene–Pliocene hiatus in the southern North Sea Basin (northern Belgium) revealed by dinoflagellate cysts. Geological Magazine, 147:760–776.

LOUWYE, S., J. DE CONINCK, AND J. VERNIERS. 1999. Dinoflagellate cyst stratigraphy and depositional history of Miocene and Lower Pliocene formations in northern Belgium (southern North Sea Basin). Netherlands Journal of Geosciences/Geologie en Mijnbouw, 78:31–46.

MANUM, S. B., M. C. BOULTER, H. GUNNARSDOTTIR, K. RANGNES, AND A. SCHOLZE. 1989. Eocene to Miocene palynology of the Norwegian Sea (ODP Leg 104), p. 611–662. *In* O. Eldholm, J. Thiede, E. Taylor, et al., Proceedings of the Ocean Drilling Program, Scientific Results, 104, Ocean Drilling Program, College Station, Texas.

MARRET, F. AND S. Y. KIM. 2009. *Operculodinium aguinawense* sp. nov., a dinoflagellate cyst from the Late Pleistocene and recent sediments of the east equatorial Atlantic Ocean. Palynology, 33:125–139.

MARRET, F., S. LEROY, F. CHALIÉ, AND F. GASSE. 2004. New organic-walled dinoflagellate cysts from recent sediments of Central Asian seas. Review of Palaeobotany and Palynology, 129:1–20.

MATSUOKA, K. 1983. Late Cenozoic dinoflagellates and acritarchs in the Niigata District, central Japan. Palaeontographica, Abteilung B, 187:89–154.

MATSUOKA, K. 1990. *Protoceratium reticulatum* (CLAPARÈDE ET LACHMANN) BÜTSCHLI, p.110–111. *In* Y. Fukuyo, H. Takano, M. Chihara, and K. Matsuoka (eds.), Red Tide Organisms in Japan–An Illustrated Taxonomic Guide. Uchida Rokakuho.

MATSUOKA, K., A. MCMINN, AND J. H. WRENN. 1997. Restudy of the holotype of *Operculodinium centrocarpum* (Deflandre & Cookson) Wall (Dinophyceae) from the Miocene of Australia, and the taxonomy of related species. Palynology, 21:19–33.

MATSUOKA, K., P. PHOLPUNTHIN, AND Y. FUKUYO. 1998. Is the archeopyle of *Tuberculodinium vancampoae* (Rossignol) (Gonyaulacales, Dinophyceae) on the hypocyst? Paleontological Research, 2:183–192.

MCKENZIE, J.A., S. SPEZZAFERRI, A. ISERN. 1999. The Miocene-Pliocene Boundary in the Mediterranean Sea and Bahamas: Implications for a Global Flooding Event in the Earliest Pliocene. Memorie Società Geologica Italiana, 54:93–108.

MELIM, L.A., H. WESTPHAL, P.K. SWART, G.P. EBERLI, AND A. MUNNECKE. 2002. Questioning carbonate diagenesis paradigms: evidence from the Neogene of the Bahamas. Marine Geology, 185:27-53.

MERTENS, K. N., B. DALE, M. ELLEGAARD, I.-M. JANSSON, A. GODHE, A. KREMP, AND S. LOUWYE. 2011. Process length variation in cysts of the dinoflagellate *Protoceratium reticulatum*, from surface sediments of the Baltic–Kattegat–Skagerrak estuarine system: a regional salinity proxy. Boreas, 40:242–255.

MUDIE, P.J. 1987. Palynology and dinoflagellate biostratigraphy of Deep Sea Drilling Project Leg 94, sites 607 and 611, North Atlantic Ocean, p. 785–812. *In* W.F. Ruddiman, R.B. Kidd, J.G. Baldauf, B.M. Clement, J.F. Dolan, et al., Deep Sea Drilling Project, Initial Reports, 94, U.S. Government Printing Office, Washington D.C.

MUDIE, P.J. 1989. Palynology and dinocyst biostratigraphy of the late Miocene to Pleistocene, Norwegian Sea; ODP Leg 104, Sites 642 and 644, p. 587–610. *In* O. Eldholm, J. Thiede, E. Taylor, C. Barton, K.R. Bjorklund, et al., Proceedings of the Ocean Drilling Program, Scientific Results, 104. Ocean Drilling Program, College Station, Texas.

MULLINS, H. T., A. C. NEUMANN, R. J. WILBER, A. C. HINE, AND S. J. CHINBURG. 1980. Carbonate sediment drifts in northern Straits of Florida. AAPG Bulletin, 64:1701–1717.

MUNSTERMAN, D.K., AND H. BRINKHUIS. 2004. A southern North Sea Miocene dinoflagellate cysts zonation. Netherlands Journal of Geosciences/Geologie en Mijnbouw, 83:267-285.

MURRAY, G. AND F. WHITTING. 1899. New Peridiniaceae from the Atlantic. Linnean Society of London, Transactions, Botany, series 2, 5(9):321–342.

NEALE, J. W. AND W. A. S. SARJEANT. 1962. Microplankton from the Speeton Clay of Yorkshire. Geological Magazine, 99:439–458.

PAULSEN, O. 1907. The Peridiniales of the Danish waters. Meddelelser fra Kommissionen for Havundersøgelser, Serie Plankton, 1(5):1–26.

PASCHER, A. 1914. Über Flagellaten und Algen. Berichte der Deutschen Botanischen Gesellshaft, 36:136–160.

PEARCE, M. A. 2010. New organic-walled dinoflagellate cysts from the Cenomanian to Maastrichtian of the Trunch borehole, UK. Journal of Micropalaeontology, 29:51–72.

PIASECKI, S. 1980. Dinoflagellate cyst stratigraphy of the Miocene Hodde and Gram formations, Denmark. Geological Society of Denmark Bulletin, 29:53–76.

PIASECKI, S. 2003. Neogene dinoflagellate cysts from Davis Strait, offshore West Greenland. Marine and Petroleum Geology, 20:1075–1088.

POULSEN, N.E., S.B. MANUM, G.L. WILLIAMS, AND M. ELLEGAARD. 1996. Tertiary dinoflagellate biostratigraphy of Sites 907, 908 and 909 in the Norwegian-Greenland Sea. p. 255-287. *In* J. Thiede, A.M. Myhre, J.V. Firth, N. Ahagon, K.S. Black, et al., Proceedings of the Ocean Drilling Program, Scientific Results, 151. Ocean Drilling Program, College Station, Texas.

RAFFI, I., J. BACKMAN, E. FORNACIARI, H. PÄLIKE, D. RIO, L. LOURENS, AND F. HILGEN. 2006. A review of calcareous nannofossil astrobiochronology encompassing the past 25 million years. Quaternary Science Reviews, 25:3113–3137.

REIJMER, J.J.G., C. BETZLER, D. KROON, R. TIEDEMANN, AND G.P. EBERLI. 2002. Bahamian carbonate platform development in response to sea-level changes and the closure of the Isthmus of Panama. Geologishe Rundschau–International Journal of Earth Sciences, 91, 482–489.

REINECKE, P. 1967. *Gonyaulax grindleyi* sp. nov.: a dinoflagellate causing a red tide at Elands Bay, Cape Province, in December 1966. Journal of South African Botany, 33:157–160.

REUNING, L., J.J.G. REIJMER, AND C. BETZLER. 2002. Sedimentation cycles and their diagenesis on the slope of a Miocene carbonate ramp (Bahamas, ODP Leg 166). Marine Geology, 185:121–142.

REUNING, L., J.J.G. REIJMER, C. BETZLER, A. TIMMERMANN, AND S.STEPH. 2006. Sub-Milankovitch cycles in periplatform carbonates from the early Pliocene Great Bahama Bank. Paleoceanography, 21:1–11.

RICCARDI, M., F. GUERRINI, F. RONCARATI, A. MILANDRI, M. CANGINI, S. PIGOZZI, E. RICCARDI, A. CEREDI, P. CIMINIELLO, C. DELL'AVERSANO, E. FATTORUSSO, M. FORINO, L. TARTAGLIONE, AND R. PISTOCCHI. 2009. *Gonyaulax spinifera* from the Adriatic sea: Toxin production and phylogenetic analysis. Harmful Algae 8:279–290.

ROCHON, A., P. J. MUDIE, A. E. AKSU, AND H. GILLESPIE. 2002. *Pterocysta* gen. nov.: A new dinoflagellate cyst from Pleistocene glacial-stage sediments of the Black and Marmara seas. Palynology, 26:95–105.

ROCHON, A., A. DE VERNAL, J.-L. TURON, J. MATTHIESSEN, AND M. J. HEAD. 1999. Distribution of recent dinoflagellate cysts in surface sediments from the North

Atlantic Ocean and adjacent seas in relation to sea-surface parameters. American Association of Stratigraphic Palynologists, Contributions Series, 35:1–152.

RÖDER, K., F. M. HANTZSCHE, C. GEBÜHR, C. MIENE, T. HELBIG, B. KROCK, M. HOPPENRATH, B. LUCKAS, AND G. GERDTS. 2012. Effects of salinity, temperature and nutrients on growth, cellular characteristics and yessotoxin production of *Protoceratium reticulatum*. Harmful Algae, 15:59–70.

ROSSIGNOL, M. 1962. Analyse pollinique de sédiments marins quaternaires en Israël. II. Sédiments pléistocènes. Pollen et Spores, 4:121–148.

SALDARRIAGA, J. F., F. J. R. TAYLOR, T. CAVALIER-SMITH, S. MENDEN-DEUER, AND P.J. KEELING. 2004. Molecular data and the evolutionary history of dinoflagellates. European Journal of Protistology, 40:85–111.

SCHILLER, J. 1936. Dinoflagellatae (Peridineae) in monographischer Behandlung. 2. Teil, Lieferung 3. *In*: Kolkwitz, R., Zehnter Band. Flagellatae. *In* Dr. L. Rabenhorst's Kryptogamen-Flora von Deutschland, Österreich und der Schweiz. Leipzig, Akademische Verlagsgesellschaft, p. 321–480.

SCHÜTT, F. 1895. Die Peridineen der Plankton-Expedition. *In* Ergebnisse der Plankton-Expedition der Humboldt-Stiftung, Bd IV (M. a. A.), Lipsius and Teicher, Kiel: 1–170, pl. 1–27.

SHIPBOARD SCIENTIFIC PARTY. 1997. Leg synthesis: Sea-level changes and fluid flow on the Great Bahama Bank slope, p. 13–22. *In* G. P. Eberli, P. K. Swart, M. J. Malone, et al., Proceedings of the Ocean Drilling Program, Initial Reports, 166, Ocean Drilling Program, College Station, Texas.

SLUIJS, A., J. PROSS, AND H. BRINKHUIS. 2005. From greenhouse to icehouse; organic-walled dinoflagellate cysts as paleoenvironmental indicators in the Paleogene. Earth-Science Reviews, 68:281-315.

STEIDINGER, K. A., AND K. TANGEN. 1996. Chapter 3: Dinoflagellates, p. 387–584. *In* C. R. Tomas (ed.), Identifying Marine Diatoms and Dinoflagellates. Academic Press Inc., San Diego, California.

STEIN, F. R. VON. 1883. Der Organismus der Infusionsthiere nach eigenen Forschungen in systematischer Reihenfolge bearbeitet. III Abteilung. II. Hälfte. Die Naturgeschichte der arthrodelen Flagellaten. Wilhelm Engelmann, Leipzig, 30 p., 25 pl.

TAYLOR, F. J. R. 1976. Dinoflagellates from the International Indian Ocean Expedition: A report on material collected by the R.V. "Anton Bruun" 1963–1964. Bibliotheca Botanica, 132, p. 1–234 and 46 pl.

TAYLOR, F. J. R. 1980. On dinoflagellate evolution. BioSystems, 13:65–108.

TRAVERSE, A. AND GINSBURG, R.N. 1967. Pollen and associated microfossils in the marine surface sediments of the Great Bahama Bank. Review of Palaeobotany and Palynology, 3:243-254.

VON STOSCH, H. A. 1969. Dinoflagellaten aus der Nordsee I. Über *Cachonina niei* Loeblich (1968), *Gonyaulax grindleyi* Reinecke (1967) und eine Methode zur Darstellung von Peridineenpanzern. Helgoländer wissenschaftliche Meeresuntersuchungen, 19:558–568.

WADE, B. S., P. N. PEARSON, W. A. BERGGREN, AND H. PÄLIKE. 2011. Review and revision of Cenozoic tropical planktonic foraminiferal biostratigraphy and calibration

to the geomagnetic polarity and astronomical time scale. Earth-Science Reviews, 104:111–142.

WAILES, G. H. 1939. Canadian Pacific Fauna. 1. Protozoa, 1e. Mastigophora. The University of Toronto Press for the Fisheries Research Board of Canada, 45 pp.

WALL, D. 1967. Fossil microplankton in deep-sea cores from the Caribbean Sea. Palaeontology, 10:95–123.

WALL, D. AND B. DALE. 1966. "Living fossils" in western Atlantic plankton. Nature, 211:1025–1026.

WALL, D. AND B. DALE. 1968. Modern dinoflagellate cysts and evolution of the Peridiniales. Micropaleontology, 14:265–304.

WALL, D., B. DALE, AND K. HARADA. 1973. Descriptions of new fossil dinoflagellates from the Late Quaternary of the Black Sea. Micropaleontology, 19:18–31.

WARNY, S. A. AND J. H. WRENN. 1997. New species of dinoflagellate cysts from the Bou Regreg core: a Miocene–Pliocene boundary section on the Atlantic coast of Morocco. Review of Palaeobotany and Palynology, 96:281–304.

WESTPHAL, H., M.J. HEAD, AND A. MUNNECKE. 2000. Differential diagenesis of rhythmic limestone alternations supported by palynological evidence. Journal of Sedimentary research, 70:715-725.

WILLIAMS, G.L. AND J.P BUJAK. 1977. Cenozoic palynostratigraphy of offshore eastern Canada. American Association of Stratigraphic Palynologists Contributions Series, 5A:14–47.

WOLOSZYNSKA, J. 1929. Dinoflagellatae der polnischen Ostsee sowie der an Piasnica gelegenen Sümpfe. Archives d'Hydrobiologie et d'Ichthyologie, 3:250–278, pl. 2–15 [Imprinted 1928]

WRENN, J.H. AND J.P. KOKINOS. 1986. Preliminary comments on Miocene through Pleistocene dinoflagellate cysts from De Soto Canyon, Gulf of Mexico. American Association of Stratigraphic Palynologists Contributions Series, 17: 169– 225.

WRIGHT, J. D. AND D. KROON. 2000. Planktonic foraminiferal biostratigraphy of Leg 166, p. 3–12. *In* P. K. Swart, G. P. Eberli, M. J. Malone, and J. F. Sarg (eds.), Proceedings of the Ocean Drilling Program, Scientific Results, 166, Ocean Drilling Program, College Station, Texas.

ZEGARRA, M. AND J. HELENES. 2011. Changes in Miocene through Pleistocene dinoflagellates from the Eastern Equatorial Pacific (ODP Site 1039), in relation to primary productivity. Marine Micropaleontology, 81:107-121.

ZEVENBOOM, D. 1995. Dinoflagellate cysts from the Mediterranean Late Oligocene and Miocene. PhD thesis. State University of Utrecht and CIP-Gegevens Koninklijke Bibliotheek, Den Haag, 221 pp.

ZONNEVELD, K. A. F., F. MARRET, G. J. M. VERSTEEGH, K. BOGUS, S. BONNET, I. BOUIMETARHAN, E. CROUCH, A. DE VERNAL, R. ELSHANAWANY, L. EDWARDS, O. ESPER, S. FORKE, K. GRØSFJELD, M. HENRY, U. HOLZWARTH, J.-F. KIELT, S.-Y. KIM, S. LADOUCEUR, D. LEDU, LIANG CHEN, A. LIMOGES, L. LONDEIX, S.-H. LU, M. S. MAHMOUD, G. MARINO, K. MATSUOKA, J. MATTHIESSEN, D. C. MILDENHAL, P. MUDIE, H. L. NEIL, V. POSPELOVA, YUZAO QI, T. RADI, T. RICHEROL, A. ROCHON, F. SANGIORGI, S. SOLIGNAC, J.-L. TURON, T. VERLEYE, YAN WANG, ZHAOHUI WANG,

AND M. YOUNG. 2013. Atlas of modern dinoflagellate cyst distribution based on 2405 datapoints. Review of Palaeobotany and Palynology, in press.

APPENDIX 1

Raw Palynological Counts of Ocean Drilling Program Site 1007 (Bahamas Platform)

ODP Site 1007, Bahamas Platform — DINOFLAGELLATE CYSTS

Series / Subseries		Planktonic foraminiferal zone	Calcareous nannofossil zone	Hole 1007B/C	Sample (core, section, interval in cm)	Depth (meters below sea floor)	Age	*Achomosphaera/Spiniferites spp.*	*Ataxiodinium zevenboomi*	*Batiachasphaer micropapillata/minuta*	*Batiachasphaera sphaerica*	*Batiachasphaera* sp.1	*Batiachasphaera/Pyxidinopsis* complex	*Bitectactodinium*? sp.1	*Bitectatodinium raedwaldii* sensu lato	*Cannosphaeropsis*? sp. 1	*Capisocysta* spp.	*"Cerebrocysta cassinascoensis"*	*Cerebrocysta* spp.	cf. *Ectosphaeropsis burdigalensis*	*Cleistosphaeridium* spp./*Glaphyrocysta reticulosa* Group	*Cleistosphaeridium placacanthum*	*Criboperidinium tenuitabulatum*	Cysts of *Pentapharsodinium dalei*	Cysts of *Protoceratium reticulatum*	Cysts of *Scrippsiella trifida*	*Dalella* cf. *chathamensis*	*"Dalella sicilensis"*	*Dapsilidinium pseudocolligerum*	*Dapsilidinium*? sp.1	*Desotodinium wrennii*	Dinocyst Type III of Core 8R	*Distatodinium paradoxum*	*Edwardsiella sexispinosa*	*Geonettia* spp.	*Gramocysta verricula*	*Hafniasphaera* sp.1	*Heteraulacysta* sp.A of Costa & Downie (1979)
PLEISTOCENE	Lower	N22	NN19	B	3H-3, 045–047	22.45	1398.76	134															1				9									
				B	4H-2, 044–046	30.44	1538.49	284																				1									
				B	5H-2, 091–093	42.41	1704.77	195	1						1													1	1								
				B	6H-1, 115–116.6	50.65	1869.31	116							1													8									
			NN16–NN18	B	7H-1, 085–087	58.35	2413.69	168		1					1													1									
				B	8H-1, 097–099	67.97	2461.07	145							2													4									
				B	9H-5, 085–086	83.35	2536.82	151	1	1					1		1							15				1	6								
				B	10H-2, 065–068	86.85	2554.05	71																					5								
				B	11X-2, 093–095	94.13	2589.91	89							1													3									
PLIOCENE	Upper	N21		B	13X-CC, 025–026	110.85	2672.25	65	3																												
				B	15X-3, 134–135.5	133.84	2785.48	55																				1									
				B	17X-5, 130.5–132	157.40	2901.52	242	1								2							2				1									
				B	19X-1, 104–106	167.14	2949.49	31							1									7							1							
				B	20X-CC, 001–002	175.42	2990.27	61	1						1		1											1			1		1				
				B	21X-CC, 029–031	184.99	3037.4	60	1															2													
	Lower	N19	NN14–NN15	B	23X-4, 095–096	208.55	4423.97	194							1									5				28								4	
				B	24X-4, 117–118.5	218.07	4498.15	133																	1			17									
				B	25X-5, 081–082	228.31	4577.94	168		1							1							2	1			20								1	
				B	26X-5, 054–055	237.14	4646.74	135	1	1			1		2									1				24	1							6	
				B	27X-4, 102–103.5	245.32	4710.48	205		1					3		1							3				9	1							1	
				B	28X-3, 130.5–132	253.41	4773.52	219		2							1							14				20								1	
				B	30X-3, 144–145	272.14	4919.46	210		1														18				16									
		N17–N19		B	31X-1, 008–009	276.98	4957.17	174		1					1		1							43	1			22		1							
?		?	?	B	32X-2, 068–070	288.19	5054.98	169		1							1							35				11	2								
MIOCENE	Upper	N16	NN11	B	34X-1, 003–005	304.33	5471.91	119																52				5							6		
				C	3R-1, 060.5–062	321.85	5924.49	171		3														5				6			1				1		
				C	4R-2, 005–007	332.10	8738.63																														
			NN10	C	7R-1, 120–123	360.80	9008.41	35		1				1										6				1			1						
				C	8R-1, 129–132	370.59	9100.44	50		2			1											15				1			1				6		
				C	9R-1, 001–004	378.91	9178.65																														
				C	10R-1,108-113	389.60	9279.13	141		2			1			1								1				8								1	
				C	11R-1,130-134	399.40	9371.25	76		1														4				3									
				C	12R-2, 010–015	408.70	9458.67	13																1				2								1	
				C	13R-1, 043–046	417.83	9544.5	85																8				6							1		
			NN9	C	15R-1, 043–046	437.13	9759.61	89						1			1							18			1	5							1		
				C	19R-1, 070–073	475.90	10439.62	93										1						4													
		N14	NN8																																		
		N13		C	25R-2, 145–150	535.80	11600.15	10			1													1													
	Middle	N12	NN7	C	26R-1, 071–074.5	543.21	11715.96																														
				C	27R-1, 031–034	552.41	11791.08	80																7				22							1	2	
				C	28R-1, 087–090	562.67	11874.85	32																1				1									
				C	30R-1, 015–018	581.15	12025.73	33			1													3				7									
				C	32R-1, 073–076	600.93	12187.23	112																28				3									
				C	37R-1, 048–051	648.78	12577.91	87																11				6									
				C	43R-1, 012–015	706.12	13046.07	82																1				4									
				C	45R-1, 016–019	725.36	13203.16	95																5				11									
		N11	NN6	C	50R-1, 124–129	774.50	13402.47	39			2		2											2				1									
				C	51R-1, 094–097	783.94	13595.63	93																1													
		N10		C	52R-3, 132–137	793.24	13895.08	72																				1									
		N9	NN5																																		
				C	54R-2, 000–004	813.30	14617.79	67										1																	2			
		N8		C	57R-1, 012–015	840.82	14802.22	40											1																			
				C	61R-1, 000–005	879.10	15514.3	33														1						3									
	Lower	N7	NN4	C	63R-2, 146–149	901.20	16128.49	4														1															
		N6		C	66R-3, 147–152	931.60	17604.3	43													2			4														
				C	68R-2, 000–005	948.00	17773.01	46			8													1	4												1	
				C	70R-1, 014–019	965.80	17956.13	124			1													11										1	2			
			NN3																																		
		N5	NN2	C	76R-2, 003–008	1025.00	19335.23	15																3													1
				C	78R-4, 135–140	1048.70	19782.27	82			1											1	12	2													1
				C	80R-4, 000–005	1065.80	20104.83	58			5											1	2														
				C	82R-2, 005–009	1082.80	20425.49	48															1														
				C	84R-6, 000–005	1107.60	22253.87	55				10							2																		
		N4	NN1	C	86R-3, 136–141	1123.80	22880.24	152			1									2			5											1			
OLIGOCENE	Upper			C	88R-5, 000–005	1144.90	23079.66	81			1							1		1	1		6					1					1				
				C	90R-1, 128–133	1159.70	23219.54	82			1		1										4														
				C	92R-1, 012–017	1177.80	23390.6	133					1								1		4					3									
				C	94R-2, 000–005	1198.20	23583.41	14																													
				C	95R-1, 049–052	1206.99	23666.49	14																													
		P22	NP25	C	96R-3, 009–013	1218.10	23771.49	22																													
				C	97R-1, 080–083	1226.60	23851.83	3																													

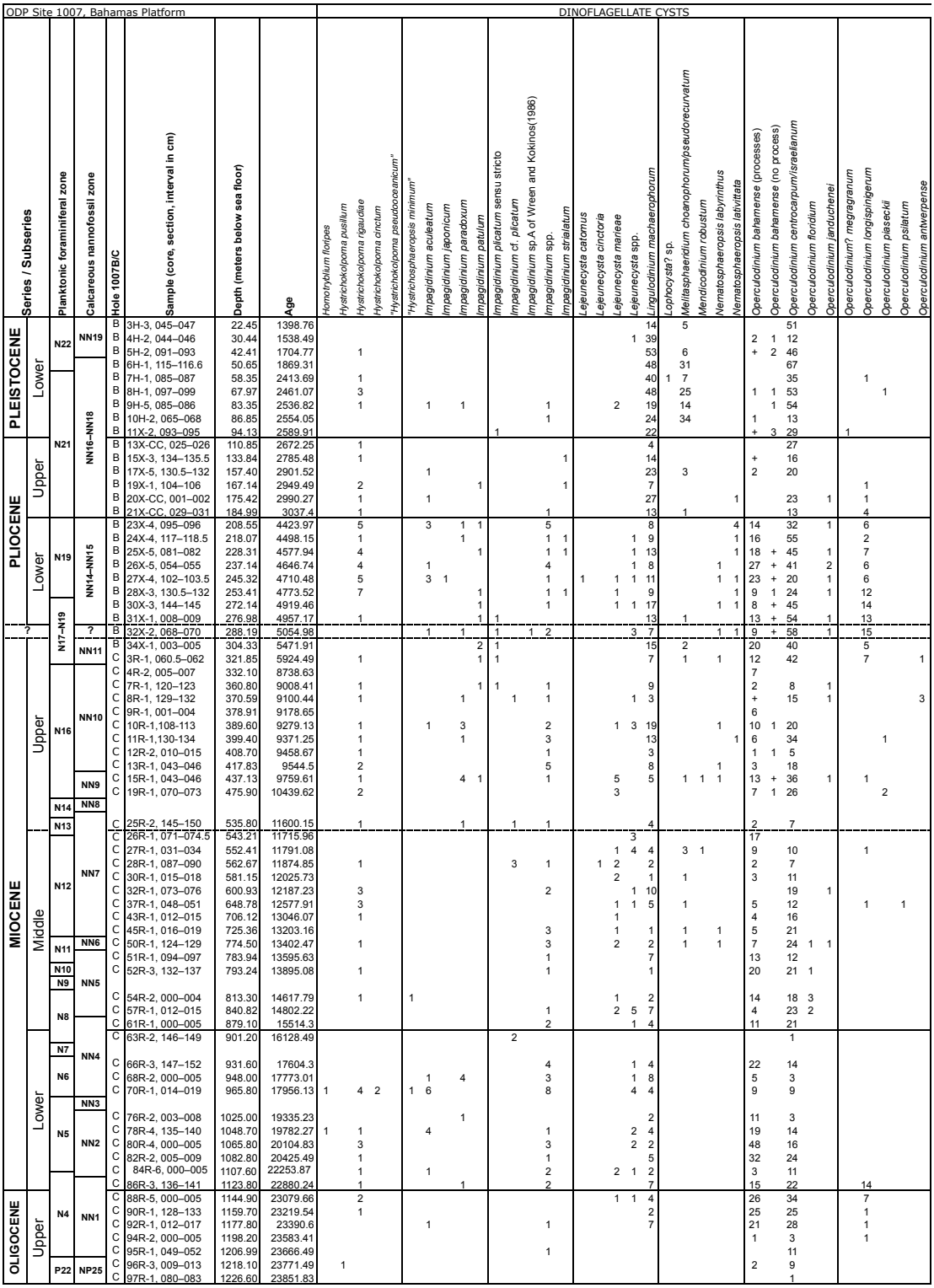
ODP Site 1007, Bahamas Platform
DINOFLAGELLATE CYSTS
Series / Subseries
Planktonic foraminiferal zone
Calcareous nannofossil zone
Hole 1007B/C
Sample (core, section, interval in cm)
Depth (meters below sea floor)
Age
Homotryblium floripes
Hystrichokolpoma pusillum
Hystrichokolpoma rigaudiae
Hystrichokolpoma cinctum
"Hystrichokolpoma pseudocoscinum"
"Hystrichosphaeropsis minimum"
Impagidinium aculeatum
Impagidinium japonicum
Impagidinium paradoxum
Impagidinium patulum
Impagidinium plicatum sensu stricto
Impagidinium cf. plicatum
Impagidinium sp.A of Wrenn and Kokinos(1986)
Impagidinium spp.
Impagidinium strialatum
Lejeunecysta catomus
Lejeunecysta cinctoria
Lejeunecysta marieae
Lejeunecysta spp.
Lingulodinium machaerophorum
Lophocysta? sp.
Melitasphaeridium choanophorum/pseudorecurvatum
Mendicodinium robustum
Nematosphaeropsis labyrinthus
Nematosphaeropsis lativittata
Operculodinium bahamense (processes)
Operculodinium bahamense (no process)
Operculodinium centrocarpum/israelianum
Operculodinium floridium
Operculodinium janduchenei
Operculodinium? megragranum
Operculodinium longispinigerum
Operculodinium piaseckii
Operculodinium psilatum
Operculodinium antwerpense
PLEISTOCENE
Lower
Upper
PLIOCENE
Lower
Upper
?
MIOCENE
Middle
Lower
OLIGOCENE
Upper
N22
N21
N19
N17–N19
?
N16
N14
N13
N12
N11
N10
N9
N8
N7
N6
N5
N4
P22
NN19
NN16–NN18
NN14–NN15
?
NN11
NN10
NN9
NN8
NN7
NN5
NN4
NN3
NN2
NN1
NP25

| Series / Subseries | | Planktonic foraminiferal zone | Calcareous nannofossil zone | Hole 100?B/C | Sample (core, section, interval in cm) | Depth (meters below sea floor) | Age | DINOFLAGELLATE CYSTS | | |

ODP Site 1007, Bahamas Platform										ACRITARCHS AND INCERTAE SEDIS															OTHERS						SAMPLE DATA		
Series / Subseries		Planktonic foraminiferal zone	Calcareous nannofossil zone	Hole 1007B/C	Sample (core, section, interval in cm)	Depth (meters below sea floor)	Age	Acritarch sp.1	Acritarch sp.2	Acritarch sp.3	*Cyclopsiella elliptica*	*Cyclopsiella granosa*	*Cyclopsiella* sp.1	Insertae sedis 1 (5 of Core68R)	Insertae sedis 2 (6 of Core68R)	*Lavradosphaera lucifer*	*Leiosphaeridia sporigiosa*	*Nannobarbophora* cf. *walldalei*	*Nannobarbophora gedlii*	*Nannobarbophora waldalei*	Spiny small acritarchs	*Veryhachium* sp.	**Total Number of Acritarchs in situ**	Foraminiferal Linings	Copepod eggs	Calcareous Dinoflagellate Cysts	Angiosperm Pollen	Gymnosperm Pollen	Spores	Number of *Lycopodium clavatum* tablets	*Lycopodium clavatum* counted	Dry Weight (in grams)
PLEISTOCENE	Lower	N22	NN19	B	3H-3, 045–047	22.45	1398.76						1						1	3			5	62	71	5	18	1	2	395	13.00
				B	4H-2, 044–046	30.44	1538.49												3				3	69	36	2			3	127	19.80
				B	5H-2, 091–093	42.41	1704.77				1								3	3			7	47	67	1	4		2	71	13.30
				B	6H-1, 115–116.6	50.65	1869.31									1			8	1			10	82	85	5	16	1	3	293	18.60
				B	7H-1, 085–087	58.35	2413.69												30	11			41	45	77		4	1	3	308	20.70
				B	8H-1, 097–099	67.97	2461.07												2	4			6	81	32	2	5	1	2	151	16.40
				B	9H-5, 085–086	83.35	2536.82												16	37			53	47	37	1	5		3	298	18.50
				B	10H-2, 065–068	86.85	2554.05						1			1			2	1			5	8	20	3	3		1	73	9.50
				B	11X-2, 093–095	94.13	2589.91												6	22			28	41	15	+	5		3	158	18.70
PLIOCENE	Upper	N21	NN16–NN18	B	13X-CC, 025–026	110.85	2672.25												2	7			9	29	15		2		2	71	14.40
				B	15X-3, 134–135.5	133.84	2785.48						1						2	13			16	71	36		2		2	190	12.40
				B	17X-5, 130.5–132	157.40	2901.52												15	35			50	195	119	4	10	4	2	419	11.90
				B	19X-1, 104–106	167.14	2949.49												2	20			22	26	33	2	14	2	1	130	10.80
				B	20X-CC, 001–002	175.42	2990.27						1						2	33			36	12	25	+	1	1	3	64	19.70
				B	21X-CC, 029–031	184.99	3037.4												2	58			60	4	26	1	2		2	130	13.30
	Lower	N19	NN14–NN15	B	23X-4, 095–096	208.55	4423.97				5		2			1			12	55			75	83	36	2	2	2	1	161	8.70
				B	24X-4, 117–118.5	218.07	4498.15												15	30			45	96	40	5	2	3	2	79	15.65
				B	25X-5, 081–082	228.31	4577.94				2		1			1			18	52			74	55	1	61	2		1	2	111	11.60
				B	26X-5, 054–055	237.14	4646.74				1	2							9	62			74	137		78	3	2	4	2	190	16.20
				B	27X-4, 102–103.5	245.32	4710.48				3	1				3			17	141			165	74		107	1	1	1	2	121	14.35
				B	28X-3, 130.5–132	253.41	4773.52					1							12	82			95	83		67	+		1	2	151	11.60
				B	30X-3, 144–145	272.14	4919.46				1	1							10	76			88	92		135	1		2	3	151	19.70
				B	31X-1, 008–009	276.98	4957.17				1	3							13	24			41	29		54		+	1	2	114	14.95
?		N17–N19	-?	B	32X-2, 068–070	288.19	5054.98				1								13	8			22	48		56	1			3	88	18.15
MIOCENE	Upper	N16	NN11	B	34X-1, 003–005	304.33	5471.91				1	5							18	2			26	151		96	8	2	1	1	456	10.85
				C	3R-1, 060.5–062	321.85	5924.49				1								33	13			47	142		37		+		2	137	15.10
			NN10	C	4R-2, 005–007	332.10	8738.63																										
				C	7R-1, 120–123	360.80	9008.41				2								1				3	19		8	2	1	2	3	72	16.75
				C	8R-1, 129–132	370.59	9100.44				1								1				2	29		11	5		1	2	203	15.75
				C	9R-1, 001–004	378.91	9178.65																										
				C	10R-1,108-113	389.60	9279.13				1								17				18	17		29				4	88	27.05
				C	11R-1,130-134	399.40	9371.25				3								5				8	34		16				3	47	21.55
				C	12R-2, 010–015	408.70	9458.67				1								1				2	4		2				3	14	19.30
				C	13R-1, 043–046	417.83	9544.5				1								5				6	32		14				2	45	13.40
			NN9	C	15R-1, 043–046	437.13	9759.61				1								11				12	109		30				2	114	12.95
				C	19R-1, 070–073	475.90	10439.62			5		1							1				7			7				3	87	19.95
		N14	NN8																														
		N13		C	25R-2, 145–150	535.80	11600.15										2						2	5		7				3	33	21.20
				C	26R-1, 071–074.5	543.21	11715.96										129						129										
				C	27R-1, 031–034	552.41	11791.08			4	1						19						24	70		20				3	88	16.30
				C	28R-1, 087–090	562.67	11874.85				2						18		2				22	90		14				3	93	19.30
			NN7	C	30R-1, 015–018	581.15	12025.73			3							17		3				23	114		20				2	49	16.50
		N12		C	32R-1, 073–076	600.93	12187.23			1	4						13		9				27	79		25				3	319	24.35
				C	37R-1, 048–051	648.78	12577.91		1	4	1						43						49	28		30				2	41	14.20
				C	43R-1, 012–015	706.12	13046.07			1	1						53						55	39		3				3	82	20.00
				C	45R-1, 016–019	725.36	13203.16			5	2						79		6				92	65		18				3	286	20.50
		N11	NN6	C	50R-1, 124–129	774.50	13402.47			1							35	3	9				48	37		41				2	173	13.50
		N10	NN5	C	51R-1, 094–097	783.94	13595.63		3	1							3						7	48		17				2	288	11.80
		N9		C	52R-3, 132–137	793.24	13895.08			4	1							2					7	80		31				2	169	15.65
		N8		C	54R-2, 000–004	813.30	14617.79			2		1											3	75		57				1	29	7.75
				C	57R-1, 012–015	840.82	14802.22		1	10													11	229		9				3	182	22.70
				C	61R-1, 000–005	879.10	15514.3				1												1	157						2	212	17.20
	Lower	N7	NN4	C	63R-2, 146–149	901.20	16128.49		3								+						3	9		4				1	244	3.90
		N6		C	66R-3, 147–152	931.60	17604.3																	60		10				1	74	7.70
				C	68R-2, 000–005	948.00	17773.01	121	170					4	1		2	3					301	34		6				1	88	6.90
				C	70R-1, 014–019	965.80	17956.13				2	2					27						31	95		18				3	624	19.30
		N5	NN3																														
			NN2	C	76R-2, 003–008	1025.00	19335.23				1						3						4			5				1	421	3.60
				C	78R-4, 135–140	1048.70	19782.27				2	1					+						3			55				1	126	10.40
				C	80R-4, 000–005	1065.80	20104.83										+							106		11				2	97	11.00
				C	82R-2, 005–009	1082.80	20425.49		78								+						78	107		2				2	98	13.80
				C	84R-6, 000–005	1107.60	22253.87		106								18					1	125	49		1				2	468	13.20
		N4	NN1	C	86R-3, 136–141	1123.80	22880.24		43			1											44	57		44				1	147	9.40
OLIGOCENE	Upper			C	88R-5, 000–005	1144.90	23079.66		17	2		1											20	137		20				1	190	5.40
				C	90R-1, 128–133	1159.70	23219.54		1														1	102		1				1	160	4.10
				C	92R-1, 012–017	1177.80	23390.6		2		1												3	47		10				2	156	13.90
				C	94R-2, 000–005	1198.20	23583.41		25								2						27	18		5				1	390	6.20
				C	95R-1, 049–052	1206.99	23666.49																0	59						2	95	17.40
				C	96R-3, 009–013	1218.10	23771.49		51														51	2		3				2	551	12.60
		P22	NP25	C	97R-1, 080–083	1226.60	23851.83		4														4	5						2	28	12.60